Journal of Mammalogy, 99(3):624–645, 2018
DOI:10.1093/jmammal/gyy048
Version of Record, first published online May 19, 2018, with fixed content and layout in compliance with Art. 8.1.3.2 ICZN.

Geographic variation in a South American clade of mormoopid bats, *Pteronotus* (*Phyllodia*), with description of a new species

Ana C. Pavan,* Paulo E. D. Bobrowiec, and Alexandre R. Percequillo

Departamento de Ciências Biológicas, Escola Superior de Agricultura "Luiz de Queiroz" – ESALQ/Universidade de São Paulo, Piracicaba 13418-900, Brazil (ACP, ARP)
Instituto Nacional de Pesquisas da Amazônia (INPA), coordenação de Biodiversidade, Manaus 69060-001, Brazil (PEDB)
Department of Life Sciences, The Natural History Museum, London SW7 5BD, United Kingdom (ARP)

* *Correspondent: anapavan@usp.br*

The subgenus *Phyllodia* (genus *Pteronotus*) comprises 9 species ranging from the western coast of Mexico to central Brazil, including Greater and Lesser Antilles. Two of them, *Pteronotus rubiginosus* and *Pteronotus* sp. 1, form an endemic South American clade within *Phyllodia* and are reported in sympatry for several localities in Guyana, Suriname, French Guiana, and northern Brazil. We herein performed a comprehensive investigation to fully characterize the cranial variation and genetic intraspecific structuring within this clade. We also integrated genetic, morphological, and acoustic evidence to formally describe the species previously reported as *Pteronotus* sp. 1. Specimens of *P. rubiginosus* occurring in sympatry with the new species have a more distinctive cranial phenotype than those from allopatric areas, suggesting character displacement as a potential force promoting divergence by decreasing resource competition or reproductive interactions between them. Although the 2 species are sympatric in several localities, the divergence in their echolocation calls also may be promoting resource partitioning at the microhabitat level, with *P. rubiginosus* foraging in less cluttered areas and the new species restricted to more cluttered areas.

O subgênero *Phyllodia* (gênero *Pteronotus*) compreende 9 espécies que ocorrem desde a costa oeste do México até o Brasil central, incluindo Pequenas e Grandes Antilhas. Duas dessas espécies, *Pteronotus rubiginosus* e *Pteronotus* sp. 1, compõem um clado endêmico da América do Sul em *Phyllodia* e são reportadas em simpatria para diversas localidades na Guiana, Suriname, Guiana Francesa e norte do Brasil. No presente estudo nós realizamos uma investigação aprofundada para melhor caracterizar a variação craniana e estruturação genética intraespecífica dentro do clado. Nós também integramos evidências moleculares, morfológicas e acústicas para descrever formalmente a espécie previamente reportada como *Pteronotus* sp. 1. Espécimes de *P. rubiginosus* que ocorrem em simpatria com a espécies nova possuem um fenótipo craniano mais diferenciado que aqueles de áreas alopátricas, sugerindo deslocamento de caráter como uma força potencial promovendo divergência para diminuição da competição por recursos ou interações reprodutivas entre eles. Embora as duas espécies sejam simpátricas em várias localidades, a divergência em seus chamados de ecolocalização também pode estar promovendo partição de recursos em uma escala de microhabitat, com *P. rubiginosus* forrageando em áreas menos fechadas e a espécie nova restrita a áreas mais fechadas.

Key words: Amazon, character displacement, echolocation calls, integrative taxonomy, morphometrics, new species

The genus *Pteronotus* inhabits the Neotropical region, from western Mexico to central and northeastern Brazil and the Caribbean (Patton and Gardner 2008; Rocha et al. 2011; Pavan and Marroig 2017). Species of *Pteronotus* are small- to medium-sized bats, ranging from 5 to 25 g (Mancina et al. 2012; Emrich et al. 2014; López-Baucells et al. 2017). They feed primarily on insects, including a high proportion of beetles (Coleoptera) in their diet, but also on other insects in the orders Lepidoptera, Diptera, Orthoptera, Hymenoptera, Hemiptera, and Odonata (Mancina 2005; Rolfe and Kurta 2012). These bats occupy several distinct habitats along their geographic range, from open areas and dry deciduous forests to evergreen

humid forests, from sea level up to 3,000 m (Herd 1983; Patton and Gardner 2008). Some of their external morphological characters include large and plate-like lower lips, short bristle-like hairs surrounding the mouth, and funnel-shaped ears with distal pinna lanceolate; the fur is short, fine, and dense, with hairs highly varying in color from reddish or orange to dark brown, depending on the individual's molt progress (Smith 1972; Simmons and Conway 2001).

The genus diversity traditionally included 6 extant species (Smith 1972; Simmons and Conway 2001), assigned to 3 subgenera: *Pteronotus*, including *P. davyi* Gray, 1838 and *P. gymnonotus* (Wagner, 1843); *Chilonycteris*, including *P. macleayi* (Gray, 1839), *P. personatus* (Wagner, 1843), and *P. quadridens* (Gundlach, 1840); and *Phyllodia*, with the sole species *P. parnellii* (Gray, 1843). Several investigations in the last years, however, suggested cryptic diversity in the genus (Lewis-Oritt et al. 2001; Dávalos 2006; Borisenko et al. 2008; Gutiérrez and Molinari 2008), particularly in the *P. parnellii* species complex (subgenus *Phyllodia*), which is represented by multiple evolutionary lineages (Clare et al. 2011, 2013; Thoisy et al. 2014). In a recent study, Pavan and Marroig (2016) employed molecular and morphometric evidence to address a new phylogenetic hypothesis for the genus (Supplementary Data SD1). According to this study, *Pteronotus* comprises 16 extant species. Many taxa previously presumed to be species widely distributed across the continent actually represent species complexes replaced parapatrically or allopatrically by each other (see table S11 of Pavan and Marroig 2016; fig. S1 of Pavan and Marroig 2017). In this context, the subgenus *Phyllodia*, traditionally including only *Pteronotus parnellii* as its single living species (with a variable number of subspecies, accordingly to different authors—see Smith 1972 and Patton and Gardner 2008), is, therefore, composed of 9 distinct species; 8 of them have valid and available names, namely *P. parnellii* (sensu stricto), *P. pusillus* (G. M. Allen, 1917), *P. portoricensis* (Miller, 1902), *P. mexicanus* (Miller, 1902), *P. mesoamericanus* (Smith, 1972), *P. fuscus* (J. A. Allen, 1911), *P. paraguanensis* (Linares and Ojasti, 1974), and *P. rubiginosus* (Wagner, 1843). One of the lineages in this complex of cryptic species does not have an available name and was referred as *Pteronotus* sp. 1 sensu Pavan and Marroig (2016), and *Pteronotus* sp. 3 sensu Clare et al. (2013).

South America is, therefore, inhabited by 4 species of the subgenus *Phyllodia*: *P. paraguanensis*, *P. fuscus*, *P. rubiginosus*, and *Pteronotus* sp. 1 (see Pavan and Marroig 2016). *P. paraguanensis* is found only in the Peninsula de Paraguaná, on the western coast of Venezuela; this taxon was recognized as a valid species based on morphometric data (Gutiérrez and Molinari 2008) and its phylogenetic position is still unknown. *P. fuscus* is known to occur in some islands in the Lesser Antilles, Colombia, Venezuela, and 3 localities in the highlands of northwestern Guyana; this species is more closely related to the *Phyllodia* species distributed in Central America (*P. mesoamericanus* and *P. mexicanus*) than to the South American species (Supplementary Data SD1; clade 4-B of Pavan and Marroig 2016). The other 2 species from South America are *P. rubiginosus*, widely distributed in the Amazon and the Brazilian Cerrado biomes, and *Pteronotus* sp. 1, which has been found in Guyana, Suriname, French Guiana (hereafter referred to as the Guianas), and the Brazilian Amazon. These 2 species comprise an exclusively South American clade within *Phyllodia* (Supplementary Data SD1; clade 4-C of Pavan and Marroig 2016) and are reported in sympatry for several localities, being molecularly and acoustically discernible (Clare et al. 2013; Thoisy et al. 2014; Pavan and Marroig 2016; López-Baucells et al. 2017). Previous studies also suggested that these species might exhibit differences in cranial and dental measurements (Thoisy et al. 2014; López-Baucells et al. 2017), although the morphometric dataset analyzed in the mentioned studies was small, both in sample size and geographic coverage.

Therefore, a more comprehensive investigation to characterize the phenotypic variation of the 2 species of the subgenus *Phyllodia* that occur in sympatry in Guianas and Brazil is still pending, as there is consistent molecular and acoustic evidence in the literature suggesting they represent independent lineages. This is an important topic to be addressed because the lack of knowledge on the morphological variation, i.e., how to differentiate these 2 species, is precluding researchers from acknowledging the real diversity of the genus *Pteronotus* in this geographic area and correctly identifying museum vouchers. Herein, we use highly complementary molecular and morphological datasets through most of the species range to investigate more thoroughly the populational structuring and the phenotypic divergence patterns between the 2 species of the South American clade of the subgenus *Phyllodia*, *Pteronotus* sp. 1, and *P. rubiginosus*. As a result, we formally describe the unnamed species of *Pteronotus* (*Pteronotus* sp. 1 sensu Pavan and Marroig 2016; *Pteronotus* sp. 3 sensu Clare et al. 2013) and redefine the taxonomic limits of *P. rubiginosus*, integrating the mitochondrial DNA (mtDNA), morphological, and bioacoustic markers here presented as well as those previously reported in the literature (Thoisy et al. 2014; Pavan and Marroig 2016; López-Baucells et al. 2017).

Materials and Methods

Sampling.—Our molecular dataset corresponded to a fragment of 651 bp of the cytochrome oxidase I (*COI*) mitochondrial gene. It included sequences of 157 individuals belonging to the lineages of *P. rubiginosus* and *Pteronotus* sp. 1 previously published by Clare et al. (2013), Thoisy et al. (2014), Pavan and Marroig (2016), and López-Baucells et al. (2017) and available at GenBank and the Barcode of Life Data System (BOLD) (Appendix I). In addition, 11 specimens from 2 localities in Amazonas, Brazil, and 1 locality from Potaro-Siparuni, Guyana, were sequenced and added to this dataset, totaling 168 individuals. These new sequences are available at GenBank under the accession numbers MH017827–MH017837. The molecular dataset included 102 individuals also included in the morphological investigation (Appendix I).

For the morphological investigation, we examined 184 vouchers of common mustached bats sampled across the geographic range of this clade in South America, including 36

localities in the Guianas and Brazilian Amazon, where the 2 lineages were reported to occur in sympatry, and 12 localities in the Cerrado and southern Amazon of Brazil, where only populations of *P. rubiginosus* have been recorded (Fig. 1; see also Pavan and Marroig 2016). We also examined 15 specimens of *P. fuscus*, including the holotype and 3 individuals previously sequenced, to provide some morphological comparisons with *Pteronotus* sp. 1 and *P. rubiginosus* (see below, in the "Systematics" section). The specimens included in the present study are housed in the following institutions: Museu de Zoologia da Universidade de São Paulo (MZUSP), Laboratório de Mamíferos da Escola Superior de Agricultura "Luiz de Queiroz," Universidade de São Paulo (LMUSP), Instituto de Pesquisas Científicas e Tecnológicas do Estado do Amapá (IEPA), Instituto Nacional de Pesquisas da Amazônia (INPA), Museu Paraense Emílio Goeldi (MPEG), American Museum of Natural History (AMNH), Royal Ontario Museum (ROM), and Musée d'Histoire Naturelle – Genève (MHNG). The complete list of examined specimens is described in Appendix II.

To gather additional evidence for delimiting species more properly, we incorporated the bioacoustic information provided by Thoisy et al. (2014) and López-Baucells et al. (2017) for 40 specimens that we analyzed in our molecular and morphological investigation. Therefore, although we have not collected new acoustic data for the present study, some important findings of these 2 previous studies are reported in the results. Appendix I presents the correspondence between the molecular, morphometric, and bioacoustics datasets and the GenBank accession numbers of all sequences included in the molecular analysis.

Molecular data.—Total genomic DNA was extracted from ethanol-preserved tissues using the Qiagen DNeasy Blood and Tissue Kit (Qiagen, Inc., Germantown, Maryland). The amplification and sequencing of the *COI* region was performed adopting the same primers and conditions described previously (Clare et al. 2007; Borisenko et al. 2008). Sequences were assembled and checked for quality using Geneious v.9.1 (Biomatters, Ltd., Auckland, New Zealand) and aligned with the sequences already available from GenBank using MEGA7 (Tamura et al. 2013). Molecular diversity indices for both species and estimates of genetic differentiation between them were calculated by MEGA7 and DnaSP v5 (Librado and Rozas 2009). We estimated the relationships among observed haplotypes using the median-joining network algorithm (Bandelt et al. 1999) by Network 5.0 (fluxus-engineering.com). We used haplotype network results to identify fixed polymorphic sites between the species and to show intraspecific population structuring.

Morphological data.—Morphological data were collected from adults only, i.e., those having fused epiphyses of phalanges and metacarpals (Smith 1972). External and osteological characters were analyzed inter- and intraspecifically. Qualitatively, we studied facial structures, fur color, differences in foramina sizes, and variation in teeth morphology. We follow Simmons and Conway (2001) in assigning homology

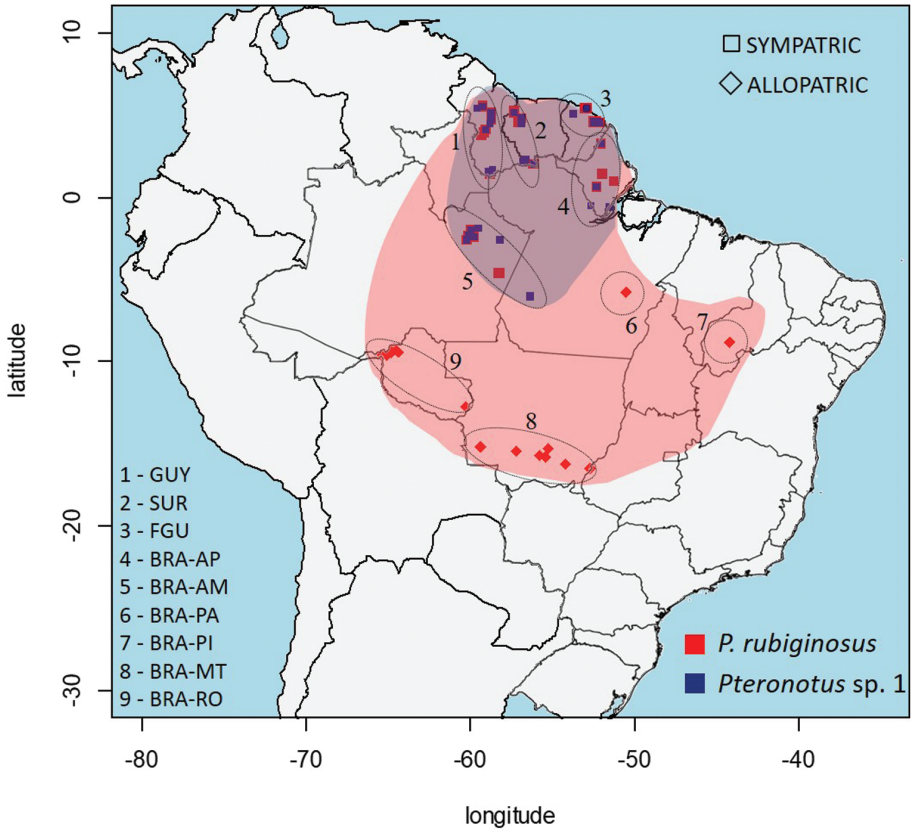

Fig. 1.——Sampling localities of the common mustached bat (*Pteronotus* cf. *rubiginosus*) included in the present study.

for the premolars and Dávalos et al. (2014) in the terminology of the dental structures evaluated in this study. Quantitatively, craniodental and mandibular measurements were recorded to the nearest 0.01 mm using digital calipers. Standard external measurements (forearm length [FL] and tibia length [TL]) are data collected in the field and were not used in the morphometric analysis. Nine linear measurements were taken from skulls and mandibles, 7 of them follow Velazco and Patterson (2014) and Nogueira et al. (2012), whereas the other 2 express the particular variation observed between these species of *Pteronotus* (Supplementary Data SD2). The measurements are:

Palatal width.—Distance across the palate, taken between the lingual margins of the alveoli of P3 at their contact with the canines.

Palatal length.—Measured from the anteriormost edge of palate bone, between the inner incisors, to its posteriormost margin, at the mesopterygoid fossa.

Greatest length of skull.—From the posteriormost point on the supraoccipital bone to the anteriormost point on the premaxilla (excludes incisors).

Interorbital breadth.—The least breadth across the postorbital constriction.

Braincase breadth.—The greatest breadth of the globular part of the braincase, excluding mastoid and paroccipital processes.

Rostral width at M2 (M2–M2).—The greatest width of the rostrum measured across the labial margins of the alveoli of M2.

Maxillary toothrow length.—The distance from the anteriormost surface of the upper canine to the posteriormost surface of the crown of M3.

Mandibular length.—Greatest length of the dentary, from its anteriormost point (excluding the incisors) to the its posteriormost point at the angular process.

Mandibular toothrow length.—Distance from the anteriormost surface of the lower canine to the posteriormost surface of m3.

To better understand the morphological variation within this clade, we initially included in these comparisons only those specimens with molecular or bioacoustic information available to support their corresponding species assignment. Localities from Guyana (GUY), Suriname (SUR), French Guiana (FGU), and from the Brazilian states of Amazonas (BRA-AM), and Amapá (BRA-AP) were treated as the overlapping area between species (Fig. 1) because these areas have reports of sympatric occurrence (Clare et al. 2013; Thoisy et al. 2014; Pavan and Marroig 2016; Lopez-Baucells et al. 2017). On the other hand, localities from the Brazilian states of Mato Grosso (BRA-MT), Pará (BRA-PA), Piauí (BRA-PI), and Rondônia (BRA-RO) were considered of exclusive occurrence of *P. rubiginosus* (Pavan and Marroig 2016; Fig. 1).

Statistical analysis.—We firstly performed a principal component analysis (PCA) to evaluate which morphological variables most contributed to the variation of each axis and, consequently, which were more informative to discriminate populations and species. This information allowed us to perform a comprehensive investigation in the complete morphological dataset (i.e., those specimens without molecular or acoustic information). To better understand how the cranial variables responded to geographic variation and differences between sexes as well as to the interaction between these 2 factors, we performed multivariate analyses of variance (MANOVA) in the complete distribution of each species. We additionally implemented MANOVA in different subsets of each species dataset to further investigate the sexual variation observed. For *P. rubiginosus*, we tested differences between sexes within one of the allopatric and sympatric populations with the largest samplings (BRA-MT and FGU, respectively) as well as for the total sampling of allopatric and sympatric regions. For *Pteronotus* sp. 1, tests were made for the largest population (FGU) and the Guianas as a whole. Divergence in variable means between sympatric and allopatric populations of *P. rubiginosus* was also tested using univariate analysis of variance (ANOVA). Discriminant function analysis (DFA) was then used to compare species across their ranges and to explore potential factors affecting the group morphometric variation, such as geographic overlap and sexual dimorphism. The PCA and MANOVA were conducted in the R software environment (R Development Core Team 2013; functions *prcomp* and *lm*, respectively). The library ggbiplot was used for the PCA graph. The ANOVA and DFA were run with SYSTAT 11.

Results

Molecular variation and population structuring.—The fragment of *COI* gene analyzed showed 80 variable positions, 29 singletons and 51 potentially parsimony informative sites, with 44 distinct haplotypes within the data. In accordance with phylogenetic data presented by previous studies (Clare et al. 2013; Thoisy et al. 2014; Pavan and Marroig 2016), the haplotype network inferred for the *COI* dataset presents 2 haplotype groups (clusters), corresponding to *P. rubiginosus* (n = 114) and *Pteronotus* sp. 1 (n = 54; Fig. 2). The K2P nucleotide divergence between them is 5.3%. As mentioned previously and highlighted in Figure 2, these 2 clusters are not entirely distinguishable by geography: there are individuals inhabiting the same or nearby localities in Guyana, Suriname, French Guiana, and northern Brazil harboring highly divergent haplotypes, although Brazilian samples from MT, RO, PA, and PI are only recovered clustered in one of the haplogroups. A minimum of 20 fixed nucleotide mutations was found setting apart these 2 clusters of haplotypes. In addition, 41 sites are polymorphic across sequences of *P. rubiginosus* but are monomorphic within *Pteronotus* sp. 1 while 22 sites show the opposite variation between the 2 species.

It is also possible to notice intraspecific structuring for both species (1.9% for *P. rubiginosus* and 0.9% for *Pteronotus* sp. 1). Most of the *P. rubiginosus* specimens (n = 72; 63%) harbor the same haplotype (HAP1) while 1–4 individuals compose the other 31 haplotypes found for this species. For *Pteronotus* sp. 1, we could find 2 haplotypes at higher frequencies (HAP2 = 27 [54%] and HAP3 = 10 [18%]) and 10 haplotypes at lower frequencies within the sampling. Molecular diversity indices and neutrality tests estimated for both species

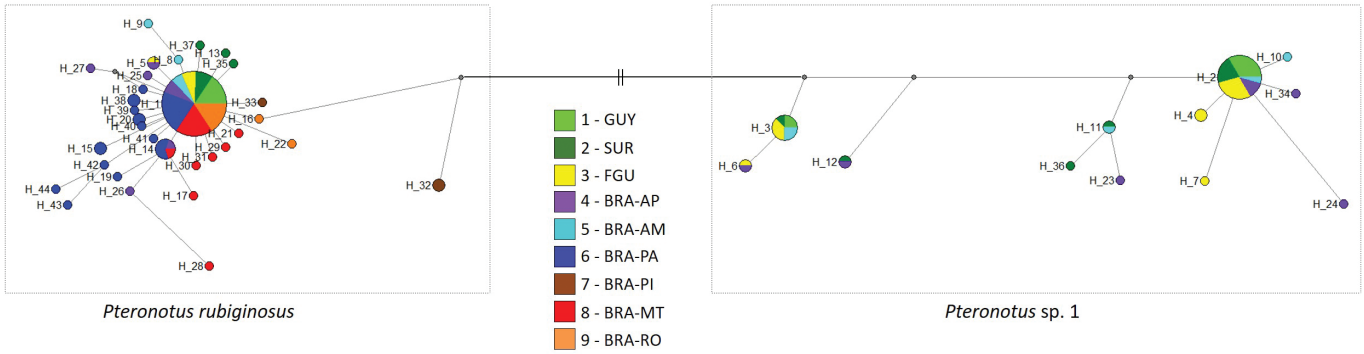

Fig. 2.——Haplotype network showing the geographic variation and intraspecific diversity in the *COI* fragment for the 2 South American sympatric species of common mustached bats (subgenus *Phyllodia*). Each haplotype found in our molecular dataset is labeled with a number. The haplotypes belonging to each cluster (representing the 2 species) differ in at least 20 mutational steps among them. Geographic samples within both species are identified by distinct colors according to the labels.

Table 1.—Molecular diversity indices and neutrality tests estimated for the *COI* region in both species. We excluded from the estimates 3 specimens with incomplete sequences and 2 specimens with uncertain assignment to species. Diversity indices presented below (Nei 1987): h = number of haplotypes; S = number of segregating sites; Hd = haplotype (gene) diversity; Pi = nucleotide diversity. Neutrality tests (significant values highlighted in bold): Tajima's D (Tajima 1989) and Fu's Fs (Fu 1997).

Species	*n*	h	Diversity indexes			Neutrality tests	
			S	Hd	Pi	D	Fs
Pteronotus rubiginosus	112	32	39	0.587	0.0018	**–2.623**	**–43.280**
Pteronotus sp. 1	51	12	22	0.686	0.0067	–0.355	–0.023

are presented in Table 1. We found a higher genetic diversity for the *COI* region in *Pteronotus* sp. 1, whereas *P. rubiginosus* seems to have gone through demographic expansion recently.

Morphometrics.—The morphometric dataset included 8 cranial measurements from 146 specimens. Table 2 describes sample sizes and mean values for selected external and cranial variables. Mean values of all cranial measurements differed among the 3 groups defined for morphometric analysis: *Pteronotus* sp. 1, *P. rubiginosus* – sympatric, and *P. rubiginosus* – allopatric; the range of values for most of these measurements, however, overlap. The result of the PCA allowed a general overview of the specimens belonging to the 2 distinct lineages in the morphospace (Fig. 3). The 1st principal component (PC1) explains ca. 86% of the total variation observed in the dataset and corresponds to size, being positively related to all 8 cranial variables; the 2nd principal component (PC2) is basically a contrast between the 2 width measurements of the cranial vault (interorbital breadth [IB] and braincase breadth [BB]) and the remaining variables, representing 4.7% of the total variation.

The PCA plot shows specimens from the same collecting localities but assigned to the distinct species in different areas of the morphospace, highlighting the dissimilarity between them. There is a general trend of size increase for both species in the northern part of their ranges (Guyana and Suriname). Specimens of *P. rubiginosus* from the allopatric (southernmost) region of the distribution (Fig. 3, populations numbered 6–9) exhibit the smallest sizes for the species and are recovered in the overlapping area of the morphometric space.

The MANOVA results suggest the presence of geographic and sexual variation for both species, but no interaction between these 2 factors (Table 3). As a general pattern, we could not observe significant differences between sexes within any of the tested populations, but we did find differences at wider geographic scales. Thus, DFA was performed for the complete dataset but also for females and males separately. Geographic variation within *P. rubiginosus* was also explored through ANOVA, which compared the populations in sympatry with *Pteronotus* sp. 1 with those in allopatry, revealing that the 8 variables are statistically different, with individuals in sympatric populations being larger on average (Supplementary Data SD3).

The DFA showed very high classification rates of specimens into the categories (species) regardless which dataset was analyzed: only females, only males, or females and males combined (Supplementary Data SD4). Therefore, we herein explore the results of the DFA performed for the complete data. More than 90% of specimens were assigned to the correct category for both species, and values described for original and jackknifed matrices are very close, highlighting the robustness of the discriminant function (DF) in differentiating the species (Klekca 1980; Pavan and Marroig 2016). Every misclassified specimen of *P. rubiginosus*, i.e., specimens belonging to *P. rubiginosus* but assigned to *Pteronotus* sp. 1 by their canonical scores, are from localities not overlapping with the range of the new species (allopatric populations of PI, MT, and RO in Brazil). When the range of DF values for each species is sorted by the different populations and modes of distribution (sympatric or allopatric), for localities of sympatry, species exhibit clear distinctive sizes, with *P. rubiginosus* exhibiting most of the size variation throughout its distribution (Fig. 4). Finally, males exhibited slightly larger values in the variable means than did females in both species, but there is no evident tendency in the DF values when both sexes are compared (data not shown).

Morphology.—We performed a careful and detailed comparative study on the skull morphology of specimens belonging

Table 2.—Measurements (mm) of the 2 external and 8 cranial variables collected from specimens of *Pteronotus* cf. *rubiginosus* according to the classification and mode of distribution established for morphometric analyses. For external measurements, mean values and sample sizes are presented. For cranial variables, samples sizes by sex (F = females; M = males; U = undetermined) and mean values (minimum–maximum range). BB = braincase breadth; GLS = greatest length of skull; IB = interorbital breadth; MdL = mandibular length; MdTL = mandibular toothrow length; MxTL = maxillary toothrow length; PL = palatal length; PW = palatal width.

Measurement	*Pteronotus rubiginosus*		*Pteronotus* sp. 1
	Allopatric	Sympatric	
Forearm length, mean (*n*)	62.8 (24)	64.9 (18)	61.6 (28)
Tibial length, mean (*n*)	25.5 (24)	26.2 (08)	24.4 (19)
n (cranial data)	38	49	60
	18 F, 17 M, 03 U	24 F, 24 M, 01 U	35 F, 23 M, 02 U
PW	4.28 (3.87–4.58)	4.49 (4.12–4.77)	4.20 (3.83–4.57)
PL	10.16 (9.76–10.51)	10.59 (10.06–11.20)	9.90 (9.53–10.42)
GLS	22.24 (21.4–23.11)	23.00 (22.24–23.64)	21.79 (21.11–22.59)
IB	4.39 (3.92–4.60)	4.51 (4.19–4.82)	4.60 (4.04–5.15)
BB	10.82 (10.32–11.40)	11.07 (10.13–11.45)	10.78 (10.08–11.30)
MxTL	9.67 (9.34–10)	10.09 (9.72–10.43)	9.43 (9.10–9.71)
MdL	17.04 (16.34–17.76)	17.73 (17.00–18.40)	16.73 (15.95–17.37)
MdTL	10.33 (9.96–10.70)	10.73 (10.35–11.14)	10.05 (9.55–10.40)

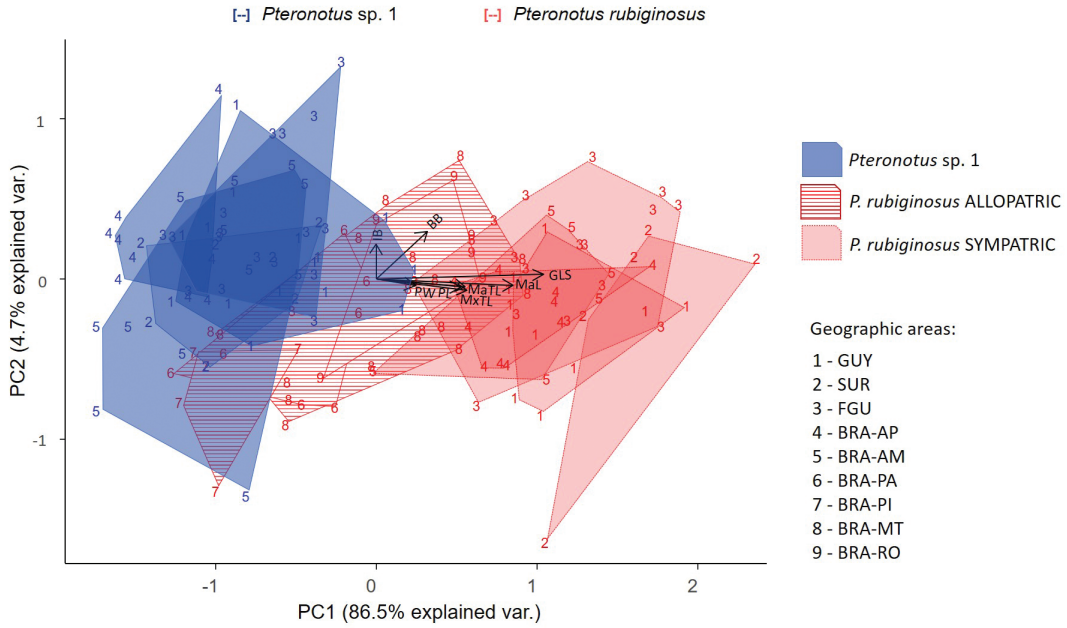

Fig. 3.—Principal component analysis displaying the cranial morphometric variation in the 2 sympatric species of the South American clade of *Phyllodia* (Clade 4C, Supplementary Data SD1). The correlation of the cranial variables with the 2 first principal components (PCs) is displayed in the center of the plot. The PC1 and PC2 correspond to 86.5% and 4.7% of the total variation, respectively. Higher values in PC1 represent larger cranial sizes while values in PC2 show variation in cranial breadth contrasted to the overall size. Numbers indicate the geographic location of individuals, whereas polygons delimit the area of each of these groups in the morphometric space.

Table 3.—Results of multivariate analysis of variance (MANOVA) performed in the complete dataset of each species (all) as well as in more restricted geographic regions within them. The *P*-values are provided in the rows, with significant values highlighted in bold. BRA-MT = Brazilian state of Mato Grosso; FGU = French Guiana.

Factor tested	*Pteronotus rubiginosus*					*Pteronotus* sp. 1	
	All	Allopatric	Sympatric	BRA-MT	FGU	All	Guianas
Sex	**2.96×10^{-4}**	**0.01**	**0.05**	0.40	0.39	**0.04**	**0.02**
Geography	**3.71×10^{-9}**	**0.01**	0.18			**3.65×10^{-4}**	0.39

to the 2 species. At first, evaluation was conducted among specimens sampled in the same or nearby localities to avoid a possible geographic bias. Further, groups of specimens were compared along the species ranges, allowing the definition of some potential informative characters to be compared between the species. We contrasted the information we had about individual identification based on previous molecular results (*COI* and cytochrome b [*Cytb*] mitochondrial genes) with

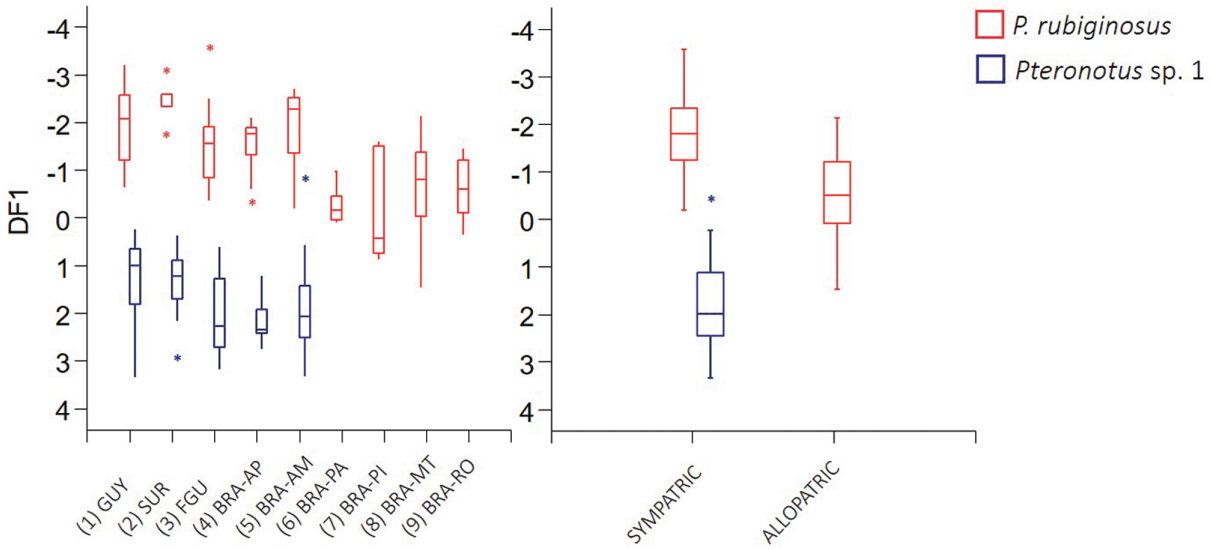

Fig. 4.—Range of the discriminant function (DF) values for the 2 species according to their geographic position or populations (left) and their mode of distribution (right). Notice the difference between the mean DF values in the populations of *Pteronotus rubiginosus* from the sympatric area of occurrence with *Pteronotus* sp. 1 (samples 1–5) and the populations from the allopatric area (samples 6–9).

the morphological data we obtained studying the specimens. We found a high correspondence between the mitochondrial clades and distinct patterns of skull morphology. The clade of *P. rubiginosus*, in general, is composed of specimens with larger skulls, with longer rostrum and palate, and proportionally smaller IB when compared to the skull of *Pteronotus* sp. 1. In addition, skulls of *P. rubiginosus* are characterized by a large pair of foramina in the pterygoid canal, which are noticeably smaller in the new species. Some morphometric traits are also useful for differentiating between the 2 species, especially the length of the maxillary toothrow (see "Systematics" section below). This set of morphological characters varies geographically, being more variable in *P. rubiginosus* than in *Pteronotus* sp. 1. For example, both species tend to have larger skulls in the northern part of their distributions (Guyana and Suriname). Furthermore, individuals of *P. rubiginosus* vary not only in skull size, but in the robustness of the rostrum across the geographic range. Populations from the southern part of the distribution (Fig. 1: allopatric area) exhibit smaller skulls with more delicate rostra. Some specimens of *P. rubiginosus* from the Guiana Shield, on the other hand, have rostra with relatively wider IB, resembling the profile of *Pteronotus* sp. 1; these specimens are noticeably large, however, and can be easily distinguished from *Pteronotus* sp. 1 occurring across this range based on skull length (Supplementary Data SD5).

The only exceptions to the pattern mentioned above were 2 specimens (MPEG 41678 and AMNH 269115) whose mitochondrial haplotypes assign them to one of the lineages while the morphological characters strongly suggest that they may belong to the other. Because a 3rd source of evidence (acoustics) was not available for these individuals, we opted for not assigning them to any of the species when investigations requiring a priori classification of the data were performed; further discussion of these specimens will be done in the following sections. We also evaluated the variation of facial structures, fur length, and color, but we found them to be uninformative for species differentiation.

Acoustic data.—Previous studies demonstrate that the 2 lineages included in this South American clade of *Phyllodia* represent 2 distinct phonic groups, which are easily discernible with no intermediate frequency values between them (Thoisy et al. 2014; López-Baucells et al. 2017). Individuals of *P. rubiginosus* emit constant frequency (CF) calls around 53 kHz in French Guiana and 55 kHz in the central Amazon, whereas *Pteronotus* sp. 1 uses CF calls between 59 and 60 kHz in the same localities. Therefore, acoustic evidence suggests that there is a consistent difference of 5–7 kHz in the echolocation calls emitted by individuals belonging to these 2 species, even at different sites, with no overlap in the peak frequency range between them (see fig. 1 of López-Baucells et al. 2017). These data also point to some level of geographical variation within each species although such variation does not compromise the ability of identifying acoustically between these 2 species in the field (López-Baucells et al. 2017). The range of values of the frequency of maximum energy (FME) in *P. rubiginosus* seems larger than that observed for *Pteronotus* sp. 1.

Systematics

Family Mormoopidae Saussure, 1860

Genus *Pteronotus* Gray, 1838

Pteronotus alitonus sp. nov.

Chilonycteris rubiginosa [*rubiginosa*]: Rehn, 1904:200; part.
Chilonycteris rubiginosa rubiginosa: Husson, 1962:74; part.
Pteronotus [*Phyllodia*] *parnellii rubiginosus*: Smith, 1972:75; part.
Pteronotus parnellii: Honacki, Kinman and Koeppl, 1982:150; part
Pteronotus sp. 3: Clare et al., 2013:14.
Pteronotus sp. 1: Pavan and Marroig, 2016:190.

Holotype.—An adult male (INPA 6942; Fig. 5), preserved in alcohol with the skull removed and cleaned, deposited at the collection of the INPA, Amazonas, Brazil. It was collected on 6 September 2014 by Ricardo Rocha (field number PP02) at the Biological Dynamics of Forest Fragments Project (BDFFP) area, 80 km north of Manaus, Brazil (2°20′S, 60°6′W, elevation of 30–125 m). Body, skull, and mandible are in good condition. Tissue is preserved in ethanol and frozen at INPA under the same ID. Sequence of the mitochondrial gene *COI* is available under the GenBank accession number MH017835.

Paratypes.—MZUSP 35505, 35523; IEPA 417, 1847; INPA 6947; ROM 98128, 106659, 117545; MHNG 1978.077, 1978.082; AMNH 267851.

Other material.—The complete list of 82 specimens of *P. alitonus* analyzed in this study is described in Appendix II.

Distribution.—The new species of *Pteronotus* is known from several localities in the pristine forests of Guyana, Suriname, French Guiana, and the Brazilian Amazon (Fig. 1; Appendix II).

Etymology.—The specific epithet, *alitonus*, is composed of the Latin words *alius* (= different, changed) and *tonus* (sound, tone), in reference to the distinct echolocation call emitted by this species in comparison to *P. rubiginosus*.

Nomenclatural statement.—A Life Science Identifier (LSID) number was obtained for the new species *Pteronotus alitonus*: urn:lsid:zoobank.org:act:4B22D88F-77BA-4021-B031-B54B946DC52D.

Historical background.—In the synonymy presented above (only with 1st use of the names), we tentatively listed authors that implicitly included in their concepts of *Chilonycteris rubiginosa* or *P. parnellii*, populations from northern Brazil and the Guianas, which could be assigned to the new species here described. The 2 latter synonyms represent not binomial (and more formal) entries, but refer to specimens whose association to this new species is clear and explicit. Several studies have been published in recent years evidencing the existence of 2 sympatric lineages of common mustached bats in the Amazonian region. Each of these studies has focused on specific questions about the group, but also provided additional sources of information to guide the present study. Based on information from 3 loci, Clare et al. (2013) described the existence of 4 distinct lineages in the continental range of the species formerly known as *P. parnellii*: 1 in Central America and 3 in South America. Two of these South American lineages, called *Pteronotus* sp. 3 and *Pteronotus* sp. 4, were found in sympatry in Guyana and Suriname. Clare et al. (2013) also described information from acoustics and morphometrics related to the geographic areas of occurrence of these lineages. Thoisy et al. (2014) showed that the 2 sympatric lineages of the *P. parnellii* complex found by Clare et al. (2013) in Guyana and Suriname were acoustically discernible and increased their ranges to French Guiana and northern Brazil. Thoisy et al. (2014) provided molecular and morphometric evidence indicating that one of these lineages (*Pteronotus* sp. 4) corresponds to *P. parnellii rubiginosus*, the taxon already known for that area. Later, Pavan and Marroig (2016) provided a new phylogenetic hypothesis and an updated taxonomic arrangement for the genus *Pteronotus.* Pavan and Marroig (2016) corroborated the existence of 8 distinct lineages within the *P. parnellii* complex (subgenus *Phyllodia*), 1 in Mexico, 1 in Central America, 3 in South America, and 3 in the Caribbean, linking them to the available names in the group (as subspecies and species names) and showing that one of the sympatric lineages from South America (*Pteronotus* sp. 1—sensu Pavan and Marroig 2016; *Pteronotus* sp. 3—sensu Clare et al. 2013) has no name available. Pavan and Marroig (2017) published a dated phylogeny for the genus *Pteronotus* based on the same molecular data published by Pavan and Marroig (2016). They discussed the historical processes related to the origin and diversification events within the group. López-Baucells et al. (2017) reported the existence of geographic variation in the echolocation calls of these 2 sympatric species of *Pteronotus* from South America. The study by López-Baucells et al. (2017) is complementary to Thoisy et al. (2014) because it showed that, despite the existence of intraspecific variation, both species are acoustically discernible, i.e., the differences are consistent across geography. They also provided additional information on the distribution of the unnamed lineage of *Pteronotus* in Central Amazon. We

Fig. 5.—Dorsal, ventral, and lateral views of the skull and ventral and lateral views of the mandible of the holotype of *Pteronotus alitonus* sp. nov. (INPA 6942). Scale bar = 5 mm. INPA = Instituto Nacional de Pesquisas da Amazônia.

hypothesize that the *Pteronotus* sp. 3 (sensu Clare et al. 2013) and *Pteronotus* sp. 1 (sensu Pavan and Marroig 2016), as well as the specimens studied by Thoisy et al. (2014) and López-Baucells et al. (2017), can be confidently recognized as the same biological entity. We advocate this as we included part of their datasets in the present appraisal and carefully compared the results.

Diagnosis.—Pteronotus alitonus is diagnosed as a distinct species by several independent characters including acoustic, molecular, and morphological data, allowing its recognition in the field, laboratory, and in scientific collections. This species can be easily identified in the field by its echolocation calls emitted between 59 and 60 KHz. *P. alitonus* has also been molecularly characterized, forming a cohesive mitochondrial clade diverging around 5% from its sister group, the species *P. rubiginosus*; the polymorphic sites between *P. alitonus* and *P. rubiginosus COI* haplotypes are described in Fig. 6. Cranially, *P. alitonus* can be distinguished by a unique combination of traits. It has a shorter rostrum, with nasals wider between the frontal and maxillary sutures, more convergent and slightly upturned at the distal part. The maxillary toothrow length (MxTL) is smaller than 9.7 mm and the IB/palatal length (PL) ratio is usually higher than 0.45. The foramina in the pterygoid canal vary from small to indistinct. The tips of upper outer incisors reach half or more of the height of upper inner incisors; they may be separated from the canines by a small gap (particularly noticeable in ventral view of the skull).

Echolocation description.—Pteronotus alitonus has duty cycle signals consisting of a short upward frequency-modulated (FM) initial component, followed by a long CF component and a short downward FM terminal component (CF-FM signal; Supplementary Data SD6). The signal has few or no harmonics and, when present, the 2nd harmonic is the most intense. The echolocation calls have an average FME of 59.2 kHz (58.4–61.5 kHz) and signal duration of 24.8 ms (7.0–40.0 ms), with great overlap between the localities recorded.

Morphological description and comparisons.—Pteronotus alitonus is a medium-sized species of mustached bat, weighting between 20 and 26 g; the FL varies from 58.8 to 64.5 mm, and the TL varies from 21.7 to 26.4 mm (López-Baucells et al. 2017; this study), usually overlapping with *P. rubiginosus* (body mass = 23–35 g; FL = 60.2–66.6 mm; TL = 22.9–27 mm). *P. alitonus* resembles the remaining species of the subgenus *Phyllodia* in external morphological characters, such as the shape of the labio-nasal plate, nostrils, tragus, size of pinnae, and patterns of dorsal and ventral fur color (Smith 1972; Simmons and Conway 2001). The pelage is dense and short (ca. 6 mm), varying from light brown and pale brown to reddish. The rostral tubercle, a dermal projection present in the proximal part of the rostrum, above the nostrils (Smith 1972; character 89 of Simmons and Conway 2001), is wide and flattened, similar to a triangle in shape. The form of this structure in some individuals from Guyana (MZUSP 35518–35528) suggests that it somehow reflects the shape of nasal bones and, as such, it seems to be wider and more swollen in *P. alitonus* when compared to *P. rubiginosus* (Supplementary Data SD7); nevertheless, a more detailed study on the variation of this character is necessary.

The skull of *P. alitonus* has a robust rostrum and a large and rounded braincase, as wide as half of the total length of the skull. Although similar to *P. rubiginosus*, it is smaller (Table 2, Fig. 7A) and exhibits a set of features that, in a combined analysis, is diagnostic for this new taxon. The nasal bones form a markedly concave area in the rostrum at the suture of the maxillary and frontal bones. Nasals also taper anteriorly, being wider in their proximal part, close to the maxillary-frontal suture, and narrower and slightly upturned in their anterior part, in the suture with pre-maxillary bones. Comparatively, the nasals in *P. rubiginosus* are more parallel and flattened throughout their extension (Fig. 7A, Supplementary Data SD5). The skull of *P. alitonus* exhibits a rectangular palate that differs from *P. rubiginosus* for being shortened in its distal portion (from premolars to incisors). The PL in *P. alitonus* rarely exceeds 10.2 mm (4 out of the 60 specimens analyzed [7%]) and the MxTL is less than 9.7 mm. *P. rubiginosus*, on the other hand, exhibits a longer rostrum: the PL equals or is larger than 10.3 mm and the MxTL is more than 9.8 mm for specimens in sympatry with *P. alitonus*. In addition, the interorbital region of *P. alitonus* is wider than in *P. rubiginosus*, the later exhibiting a more pronounced constriction (Table 2). Consequently, the estimated ratio between the IB and the PL (IB/PL) is higher in *P. alitonus* (mean = 0.46 ± 0.0184) than in *P. rubiginosus* (mean = 0.43 ± 0.0148). Most of the specimens of *P. alitonus* (88%) show the IB/PL ratio equal or greater than 0.45, whereas 83% of the *P. rubiginosus* specimens have ratios equal or below 0.44. The BB in *P. rubiginosus* (10.13–11.45 mm) is very similar to that of *P. alitonus* (10.08–11.30 mm) but seems proportionally smaller because of the larger sizes exhibited by *P. rubiginosus*. Ventrally, the pterygoid

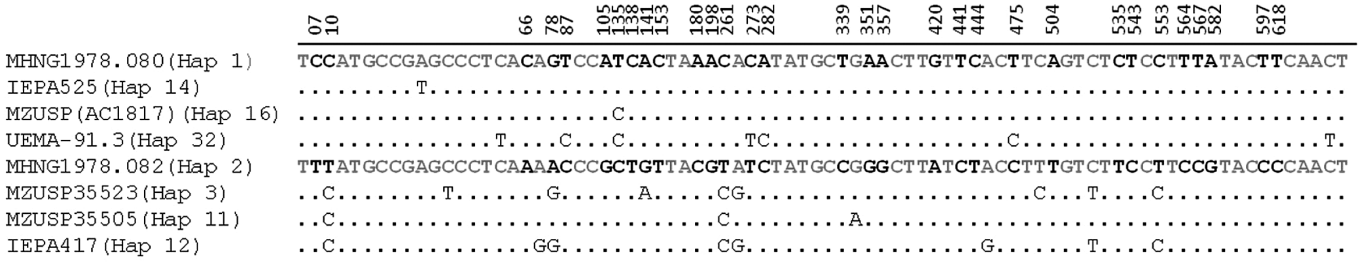

Fig. 6.—Single nucleotide polymorphisms (SNPs) among observed haplotypes of *Pteronotus rubiginosus* and *P. alitonus* sp. nov. in the 651 bp fragment of *COI* gene analyzed. Four haplotypes of each species (*P. rubiginosus*: HAP1, 14, 16, 32; *P. alitonus*: HAP2, 3, 11, 12) are shown. Fixed SNPs between the most frequent haplotype of each species (HAP1 × HAP2) are highlighted in bold.

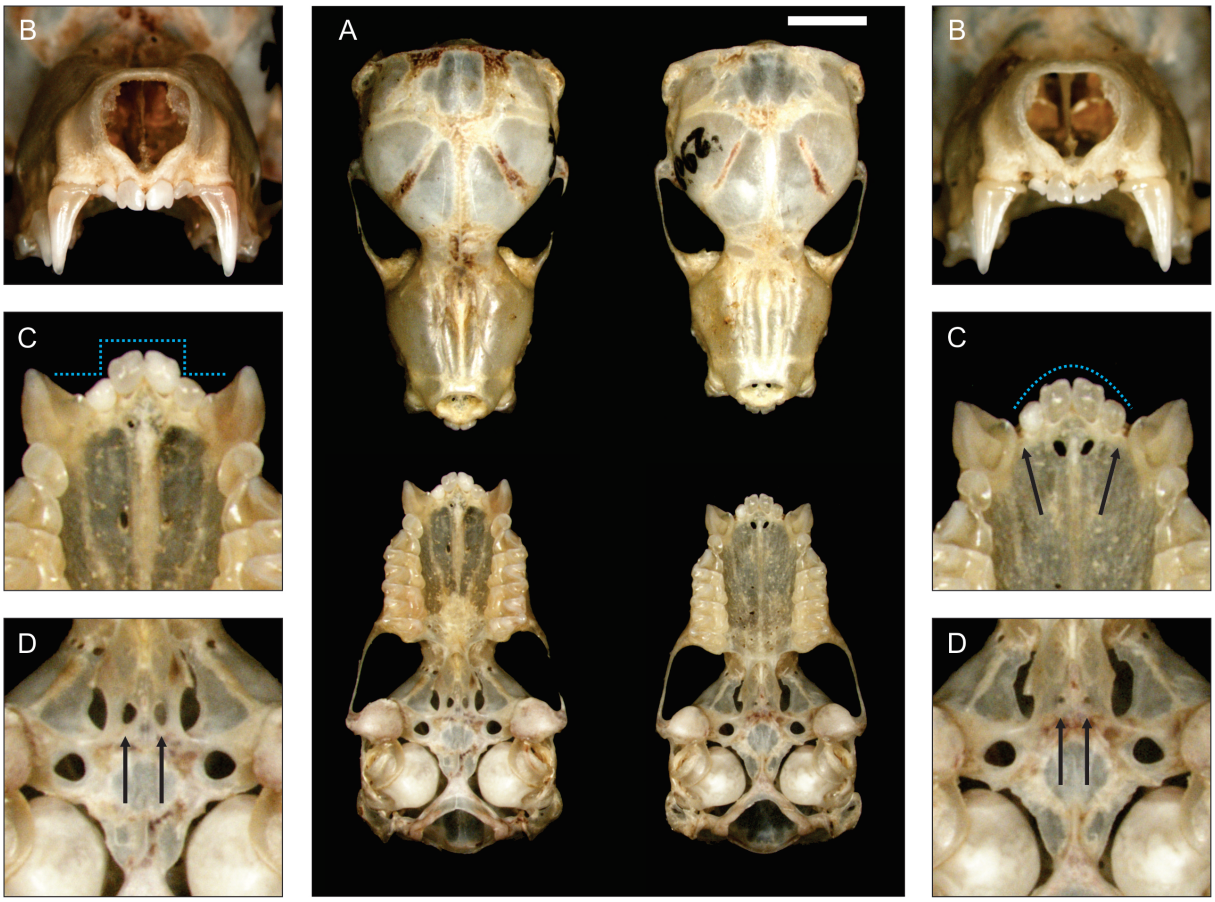

Fig. 7.—Comparison of the cranial morphology between *Pteronotus rubiginosus* (MHNG 1978.083) and *P. alitonus* sp. nov. (MHNG 1978.082) from Grotte Mathilde, French Guiana. A) Dorsal and ventral views of the skull of *P. rubiginosus* (left) and *P. alitonus* (right); B) frontal view of the skull, contrasting the sizes of the internal (I1) and external (I2) incisors in the 2 species; C) ventral view of 1st half of the palate, highlighting the form outlined by the incisors and the gap between I2 and canines in *P. alitonus*; D) ventral view of the basicranial region, with arrows indicating the foramina in the pterygoid canal with different sizes in the 2 species. Scale bar in top right of A = 5 mm. MHNG = Musée d'Histoire Naturelle – Genève.

canal has a pair of foramina varying from almost indistinct perforations to small pits (less than 1/3 of the foramen ovale) in the new species; alternatively, *P. rubiginosus* specimens exhibit a large pair of foramina, as large as half of the diameter of the foramen ovale (Fig. 7D).

The dental formula is the same as for all other mormoopids, i 2/2 c 1/1 p 2/3 m 3/3 = 34. The inner (or central) upper incisors (I1) are bilobed and usually have less than twice the height of the outer (or lateral) incisors (I2); the I1 are proportionally larger in *P. rubiginosus* than in *P. alitonus,* with more than twice the height of I2 (Fig. 7B). Ventrally, this character is also noticeable, with the margins of the incisors usually forming a continuous arc in *P. alitonus*, while the margins of the incisors are steeply uneven in *P. rubiginosus* (Fig. 7C), with the central ones forwardly projected. A small gap separating the outer upper incisors from the canines is sometimes present in *P. alitonus* (e.g., INPA 6942, MHNG 1978.082, AMNH 267851, ROM 106659) and is absent in all specimens of *P. rubiginosus*. The labial cingulum and the entire labial margin of the 1st upper premolar (P3 in homology—sensu Simmons and Conway 2001) in *P. alitonus* exhibits a concave and rounded profile (C-shaped), with deeper notches on the molar toothrow between the canine and the P3 and between the P4 and P3; by contrast, the labial cingulum of the P3 of *P. rubiginosus* exhibits a less concave, more open profile, with much less noticeable notches between P3 and the adjacent teeth. Moreover, the general shape of the P3 is usually different between species, being more rounded and narrow buccolabially in *P. alitonus* and more elongated and long buccolabially in *P. rubiginosus*. The inner lower incisors are trilobed and larger than the outer bilobed incisors in both species but for some individuals of *P. alitonus*, i1 and i2 crowns are not in contact. The 1st and 3rd lower premolars (p2 and p4) are large and have well-developed labial cingulids; in both species, the p3 is peg-like and compressed between the lingual edges of p2 and p4, although in *P. rubiginosus* it is usually larger than in *P. alitonus*.

Additional comparisons.—We examined the cranial morphology of specimens of the geographically contiguous species *P. fuscus* and compared them with specimens of *P. rubiginosus* and *P. alitonus* from Guyana to provide a few insights on

their differentiation. *P. fuscus* has its easternmost distribution in the highlands of northwestern Guyana (Clare et al. 2013), near the border with Venezuela, whereas *P. rubiginosus* and *P. alitonus* extend northward to central and southeastern Guyana (Fig. 1). So far, these 3 species have not been recorded at the same locality and, therefore, *P. fuscus* is considered to have a parapatric distribution relative to *P. rubiginosus* and *P. alitonus*. In general, specimens of *P. fuscus* have a skull shape more similar to *P. rubiginosus*, but size more similar to *P. alitonus* (Supplementary Data SD8). Comparatively, the skull of *P. fuscus* has a narrow and delicate rostrum; the nasal bones are parallel and flat. *P. fuscus* can be easily differentiated from *P. rubiginosus* based on the smaller size (greatest length of skull [GLS] = 21.4 mm ± 0.36; MxTL = 9.33 mm ± 0.2). When compared to *P. alitonus*, specimens of *P. fuscus* have noticeably narrower rostra, which are not slightly upturned in their anterior most part as for *P. alitonus*. The maxillary bones are less inflated in their suture with nasals; morphometrically, this feature is noticed by the greatest width across the molars (M2–M2), generally < 8.0 mm in *P. fuscus*, and > 8.18 mm in *P. alitonus* from Guyana.

Natural history.—Little is known about the biology or behavior of this new species, but our data suggest that it forages preferentially in highly cluttered forested areas as there are no reports on the species occurrence in more open areas such as savannas or karstic regions in the Amazon.

Remarks.—As a consequence of the description of *P. alitonus*, *P. rubiginosus* needs to be redefined. In the present study, we described several morphological features that allow the identification of *P. rubiginosus*, including quantitative and qualitative characters (see previous section; see also Table 2 and Fig. 7). *P. rubiginosus* is found in the Amazon and Cerrado biomes of South America. The occurrence of this species has been confirmed by molecular data for Guyana, Suriname, French Guiana, northern and central Brazil (and states of Maranhão and Piauí in northeastern Brazil), and Bolivia (Pavan and Marroig 2016; A. C. Pavan, pers. obs.). There are also records of *Pteronotus* cf. *rubiginosus* in the Amazonian regions of Peru, Colombia, and Venezuela but the status of these populations need to be reviewed.

Discussion

Our comparative study evaluated the existence of an unnamed evolutionary lineage of *Pteronotus* (*Pteronotus* sp. 1—sensu Pavan and Marroig 2016; *Pteronotus* sp. 3—sensu Clare et al. 2013) occurring in sympatry with *P. rubiginosus* in several localities in the Guianas and Brazilian Amazon (Clare et al. 2013; Thoisy et al. 2014; Pavan and Marroig 2016; López-Baucells et al. 2017). Using cranial, genetic, and acoustic data, we corroborate the hypothesis of a new species of *Pteronotus* and formally describe *P. alitonus*.

These 2 species, *P. rubiginosus* and *P. alitonus*, diverge in genetic and acoustic traits throughout their geographic ranges. Despite their external similarity, we herein provided skull diagnostic traits that will be useful for future identification of material in collections. We also provided some insights on their evolution and ecology, which are essential for the adequate diagnosis of the new species.

Genetic divergence and population structuring.—The *COI* haplotype network reconstruction recovers both species, *P. rubiginosus* and *P. alitonus*, as cohesive clusters, but with intraspecific structuring. Molecular diversity indexes (Table 1) point to a higher genetic diversity in *P. alitonus* compared to *P. rubiginosus*. In *P. alitonus*, the 2 most frequent haplotypes (HAP2 and HAP3) differ in 9 mutated positions from each other, with 3 intermediary haplotypes (median vectors) inferred by the analysis (Fig. 2). No spatial correlation seems to exist, however, for the distribution of these haplotypes; both are widespread across the species geographic range. *P. rubiginosus* exhibits 1 central haplotype (HAP1), surrounded by several related haplotypes at low frequency and showing little difference among them. This pattern suggests these low-frequency haplotypes originated recently and agrees with a scenario of recent demographic expansion (Wakeley 2004; Ferreri et al. 2011). This premise is confirmed by the significant values of neutrality tests found for *P. rubiginosus* (Table 1). A more divergent haplotype occurs in *P. rubiginosus* (HAP32), represented by 2 specimens near the border of Maranhão and Piauí states, northeastern Brazil, but unfortunately these specimens were not available for the morphological analyses. Alternatively, we examined other individuals from Piauí, Brazil (Appendix II), and these specimens are unequivocally assigned to *P. rubiginosus*, although exhibiting the smallest average sizes of our *P. rubiginosus* sampling.

Morphological variation and character displacement.—We corroborate previous studies (Thoisy et al. 2014; López-Baucells et al. 2017), showing that specimens of *P. rubiginosus* have larger skulls than specimens of *P. alitonus* where these species occur in sympatry. In addition, we present some cranial characters useful to distinguish between these 2 lineages, the most consistent being the foramina in the pterygoid canal. This structure exhibits distinct states (Fig. 7D): in *P. rubiginosus*, 81 out of the 87 specimens (93%) have a relatively large pair of foramina, averaging from 1/3 to 1/2 of the diameter of the foramen ovale; whereas in *P. alitonus*, approximately one-half of specimens (31 of 60) exhibit a small-sized pair of foramina (less than 1/3 of the diameter of foramen ovale) and the other half (29 of 60) exhibit foramina that are barely perceptible as perforations in the pterygoid region. We also found that the 2 species are more easily distinguishable by the ratio of PL to IB: individuals of *P. rubiginosus* usually have longer palates but proportionally narrower constrictions than *P. alitonus*.

Quantitatively, the 2 species also markedly differ in 2 measurements related to the rostrum, i.e., the length of palate and maxillary toothrow. The difference in these characters, however, is more conspicuous in sympatry. Individuals of *P. rubiginosus* are larger in areas where the species range overlaps with *P. alitonus*. Therefore, the morphological variation of specimens of *P. rubiginosus* from the allopatric area (Brazilian samples of PA, PI, MT, and RO) seems to slightly blur this clear separation, since they exhibit smaller sizes and more polymorphic

cranial characters. The DF1 values in the different populations (Fig. 4) clearly outline such a distinctive pattern. Also, most of the individuals displaying small pairs of foramina or higher IB/PL ratios (0.45) are found in the allopatric distribution of *P. rubiginosus.* Our results suggest that specimens of *P. rubiginosus* occurring in sympatry with *P. alitonus* are more dissimilar than those occurring in allopatry, at least concerning the cranial phenotype.

The difference in morphology of *P. rubiginosus* in sympatry and allopatry with *P. alitonus* agrees with character displacement theory, which hypothesizes that phenotypic differences between species are enhanced where they occur together, to minimize or avoid resource competition or reproductive interactions between them (Pfenning and Pfennig 2009). Character displacement is believed to be a ubiquitous phenomenon in nature, although difficult to test in the face of alternative hypothesis explaining divergence on closely related sympatric species (sensu Losos 2000; Pfennig and Pfennig 2009). This competitively mediated divergence can finalize a process of allopatric speciation (Pfennig and Pfennig 2010). Several criteria have been proposed to test the strength of a particular adaptive hypothesis, including that phenotypic divergence: 1) must be nonrandom, 2) has to show a genetic basis, and 3) should reflect differences in resource use (Schluter and McPhail 1992; Losos 2000). Testing for all premises is beyond the scope of the present study. Our ANOVA results, however, do reveal a significant morphological divergence between sympatric and allopatric populations of *P. rubiginosus* for all cranial characters (Supplementary Data SD3). Alternatively, half of the characters are different when allopatric populations are tested among themselves, and no significant differences are found in the variable means among the sympatric populations (data not shown). This finding seems to meet the 1st criteria, that differences are nonrandom. It also suggests a higher phenotypic variation within the more widespread species *P. rubiginosus*, especially in its allopatric range with *P. alitonus*, a factor that is expected to be present in species undergoing character displacement (Pfennig and Pfennig 2009). *P. alitonus*, on the other hand, is more conservative in its size throughout its known (smaller) range. In addition, geographic variation in the echolocation calls has also been reported for these 2 species (López-Baucells et al. 2017). It is possible that the variation in the calls of *P. rubiginosus* is even greater in its allopatric area of occurrence. However, more evidence is needed in the southernmost region of the *P. rubiginosus* distribution to test this hypothesis.

Echolocation calls and foraging behavior.—Both *P. rubiginosus* and *P. alitonus* find prey using high-duty cycle signals that consist of a long CF component followed by a short downward FM terminal component. Long CF-FM signals are associated with Doppler shift compensation and are used by bats that search for prey in narrow spaces (Schnitzler and Denzinger 2011; Denzinger and Schnitzler 2013). Pulse duration is similar in the 2 species but the FME always differ by 5–7 kHz between them (López-Baucells et al. 2017). There is a clear relationship between call frequency and the size of prey that insectivorous bats can detect. While bats calling at higher frequencies are expected to catch smaller insects with more efficiency, those emitting at lower frequencies will target larger insects more successfully (Jones 1997; Kingston et al. 2001). However, it has been discussed that small differences in the call frequencies such as the one described between *P. rubiginosus* and *P. alitonus* are not sufficient to significantly influence target specificity, and thus cannot promote resource partitioning associated with prey size (Jones and Barlow 2004; Kingston et al. 2001; Clare et al. 2013).

Alternatively, the hypothesis of competitive exclusion between these 2 species, as suggested by the cranial phenotypic traits, may be taking place spatially instead of acting on prey-size selection. Accordingly, the 2 species may search similarly for their targets, but exploit distinct microhabitats in their sympatric area of occurrence. Because *P. rubiginosus* emits calls at lower frequencies, its foraging strategy might be more associated with less cluttered environments, while the higher frequencies of *P. alitonus* increase the target detection in more cluttered areas. For example, *P. rubiginosus* crosses open areas between islands created by the Balbina hydroelectric dam, while *P. alitonus* is restricted to the continuous forest (Ponzio 2017). Also, some Amazonian localities characterized by more open and karstic landscapes (e.g., eastern Pará, Brazil) as well as the Cerrado of Brazil, a savanna-like environment, are areas where only *P. rubiginosus* occurs. This pattern seems to be more related to some specific requirement of *P. alitonus* than an actual preference of *P. rubiginosus* since the latter also forages in cluttered areas when not in sympatry with *P. alitonus* (De Oliveira et al. 2015; Ponzio 2017). Based on this observation, we hypothesize that *P. rubiginosus* may be exploiting more open habitats within the Amazon Region, such as the Amazonian savannas, whereas *P. alitonus* is mostly restricted to more cluttered microhabitats while searching for food.

Finally, distinctive patterns of microspatial segregation of these 2 species might be related to the molecular results that we observed. The lower nucleotide diversity and the large number of individuals sharing 1 single haplotype in *P. rubiginosus* may be a consequence of its high dispersal capability and, consequently, the higher gene flow among the populations. *P. alitonus* seems to exhibit a smaller geographic range and shows a greater intraspecific structuring that may reflect its foraging behavior associated with highly cluttered areas and limitations to cross open landscapes.

Inconsistencies between morphology and molecular data.—Two specimens included in our analysis presented disparities regarding molecular and morphological data. MPEG 41678 (Itaituba, Brazil) has a mitochondrial haplotype of *P. rubiginosus*; its phenotype, however, resembles *P. alitonus*, being small (FL = 58.9 mm; GLS = 21.2 mm) and exhibiting diagnostic cranial characters such as small pterygoid foramina, PL = 9.71 mm and high IB/PL ratio (0.47). AMNH 269115 (Cayenne, French Guiana), on the other hand, had a haplotype of *P. alitonus* while its cranial features mostly agree with *P. rubiginosus* (GLS = 23.5 mm; PL = 10.71 mm; IB/PL ratio = 0.44; large pterygoid foramina). Three distinct interpretations of these results are possible: 1) the defined

cranial morphological characters are not completely consistent for species differentiation, exhibiting polymorphic states for some individuals of the distinct species; 2) the mtDNA exhibits some level of incomplete lineage sorting between the species; and 3) there is ongoing gene flow between the species due to secondary contact, leading to introgression of mtDNA from one species to the other. We cannot assert which of these scenarios is the most likely without a deeper investigation including more molecular markers, preferably from independent systems.

Regarding the 1st assumption, our data show that there is variation for some of the cranial traits, including overlapping in some quantitative markers: these 2 specimens could represent outliers of our dataset, exhibiting the extreme of the variation expressed by the species molecularly delimited. On the other side, incomplete lineage sorting and interspecific gene flow (with introgression) are frequently described phenomena for recently diverged species (Degnan and Rosenberg 2009; Petit and Excoffier 2009). An event of introgression has been already reported in the genus *Pteronotus* (Pavan and Marroig 2016). One specimen of *P. gymnonotus* was found to have the mtDNA of *P. fulvus*, and these species diverged earlier than *P. alitonus* and *P. rubiginosus* (see Pavan and Marroig 2017). Therefore, introgression could be the cause of the inconsistency described above. These 2 specimens were collected in the sympatric area of occurrence of *P. rubiginosus* and *P. alitonus* but in opposite sides of this range (Cayenne = north of the sympatry zone; Itaituba = south of the sympatry zone), which means that, if introgression has caused this pattern, 2 independent events are necessary to explain the finding. In addition, the direction of the introgression would have to be different in the 2 events. Still, these phenomena do not preclude divergence in the rest of the genome, particularly if we assume that mtDNA is evolving under neutrality and, therefore, not related to the speciation process (Feder et al. 2013). Alternatively, specific cranial traits might be susceptible to evolutionary constraints due to highly specialized functions of the skull (Cheverud 1982; Santana and Lofgren 2013), such as the echolocation in high-duty cycle echolocating bats, and may be more tightly related to factors leading to reproductive isolation (Kingston et al. 2001; Clare et al. 2013). Based on this, we tentatively suggest that the disparity is being caused by conflicting information from the mtDNA, and we opted for identifying these specimens according to their phenotypes (Appendix I).

The case described above is an excellent example of how multiple sources of evidence are important for assigning individuals to species with confidence. Several studies have shown that bioacoustic data is a useful tool for the identification of bat species (Barataud et al. 2013; Thoisy et al. 2014; López-Baucells et al. 2016), and in the case of the subgenus *Phyllodia* it may be essential to understand the contact areas between species and aspects of their biology. In some cases, only morphological information is available for taxonomic studies, such as for fossils and highly endangered or extremely rare species. Nevertheless, in all other cases, an integrative approach should be attempted.

Acknowledgments

This research was supported by grants 2009/16009-1, 2015/02132-7, 2016/23565-1, and 2016/20055-1, São Paulo Research Foundation (FAPESP). We thank P. Velazco, N. Simmons, and J. Wible for the kind assistance regarding cranial anatomy. We are also thankful to S. Pavan and J. P. Hoppe for the valuable suggestions as well as to the 3 anonymous reviewers for contributing to the improvement of the manuscript. We thank J. Dallapicola, E. Fiedler, and A. Caccavo for help with pictures and E. Gutierrez for allowing us to use the drawings of Supplementary Data SD2. The following curators and collection managers provided loans of specimens: B. Lim and J. Miller (Royal Ontario Mus), F. Catzeflis and M. Ruedi (Musée d'Histoire Naturelle - Genève), I. Castro (Instituto de Pesquisas Científicas e Tecnológicas do Estado do Amapá), M. N. F. da Silva (Instituto Nacional de Pesquisas da Amazônia), M. de Vivo and J. Gualda (Museu de Zoologia da Universidade de São Paulo). ARP also acknowledges a productivity scholarship from the Brazilian National Council for Scientific and Technological Development (CNPq). This research constitutes publication number 738 in the BDFFP Technical Series.

Supplementary Data

Supplementary data are available at *Journal of Mammalogy* online.

Supplementary Data SD1.—Phylogenetic hypothesis proposed for the genus *Pteronotus* according to Pavan and Marroig (2016). The phylogeny represents a species tree estimated from 6 molecular markers, depicting the relationships among major clades according to the multispecies coalescent approach (see Pavan and Marroig 2016 for more details).

Supplementary Data SD2.—The 9 cranial and mandibular measurements taken in the present study: palatal width (PW), palatal length (PL), greatest length of skull (GLS), interorbital breadth (IB), braincase breadth (BB), greatest width of rostrum measured across the labial margins of the alveoli of M2 (M2–M2), maxillary toothrow length (MxTL), mandibular length (MaL), and mandibular toothrow length (MaTL). The M2–M2 measurement was taken from a few specimens for the comparative morphology description (systematic account) and, therefore, was not included in the morphometric analysis. Scale bar = 0.5 cm. Drawings of skull by Ivan Akirov and taken from Gutiérrez and Molinari (2008).

Supplementary Data SD3.—Average measurements in allopatric (ALLO, n = 38) and sympatric (SYM, n = 49) populations of *Pteronotus rubiginosus* and result of analysis of variance (ANOVA) between them.

Supplementary Data SD4.—Classification matrix of the discriminant function analysis (DFA) performed with all specimens of both species compared to the classification rates of the DFA performed with only females (F) or males (M).

Supplementary Data SD5.—Comparison between the new species *Pteronotus alitonus* sp. nov. (ROM117576, left) and *P. rubiginosus* (ROM 117608, right) from Suriname (Blanche Marie Vallen, Sipaliwini), showing the difference in the size and shape of the nasal bones.

Supplementary Data SD6.—Comparison between the echolocation signals emitted by *Pteronotus rubiginosus* and *P. alitonus* sp. nov. The specimens were recorded on the islands of the Balbina Hydroelectric Reservoir (BHR), a man-made reservoir within the Uatumã River basin of central Brazilian Amazonia (1°01′–1°55′S; 60°29′–59°28′W). These recordings were only used to illustrate the sonograms and were not part of the analyses since no bat was captured.

Supplementary Data SD7.—Comparison between the rostral pad (arrows) of *Pteronotus rubiginosus* (MZUSP 35519, left) and *P. alitonus* sp. nov. (MZUSP 35523, right). Both specimens are from Amaila Falls, Potaro-Siparuni, Guyana.

Supplementary Data SD8.—Comparison of the cranial morphology among the 3 species of *Phyllodia* distributed in the Guiana Shield. *Pteronotus rubiginosus* (ROM 98127, left) and *P. alitonus* sp. nov. (ROM 98128, middle) occur sympatrically in the Guianas and Brazilian Amazon, whereas *Pteronotus fuscus* (ROM 100871, right) is found in the highlands of northwestern Guyana and in Venezuela.

Literature Cited

Bandelt, H. J., P. Forster, and A. Röhl. 1999. Median-joining networks for inferring intraspecific phylogenies. Molecular Biology and Evolution 16:37–48.

Barataud, M., et al. 2013. Identification et écologie acoustique des chiroptères de Guyane française. Le Rhinolophe 19:103–145.

Borisenko, A. V., B. K. Lim, N. V. Ivanova, R. H. Hanner, and P. D. Hebert. 2008. DNA barcoding in surveys of small mammal communities: a field study in Suriname. Molecular Ecology Resources 8:471–479.

Cheverud, J. M. 1982. Phenotypic, genetic, and environmental morphological integration in the cranium. Evolution 36:499–516.

Clare, E. L., A. M. Adams, A. Z. Maya-Simões, J. L. Eger, P. D. Hebert, and M. B. Fenton. 2013. Diversification and reproductive isolation: cryptic species in the only new world high-duty cycle bat, *Pteronotus parnellii*. bmc Evolutionary Biology 13:26.

Clare, E. L., B. K. Lim, M. B. Fenton, and P. D. Hebert. 2011. Neotropical bats: estimating species diversity with DNA barcodes. PLoS ONE 6:e22648.

Clare, E. L., B. K. Lim, M. D. Engstrom, J. L. Eger, and P. D. N. Hebert. 2007. DNA barcoding of Neotropical bats: species identification and discovery within Guyana. Molecular Ecology Notes 7:184–190.

Dávalos, L. M. 2006. The geography of diversification in the mormoopids (Chiroptera: Mormoopidae). Biological Journal of the Linnean Society 88:101–118.

Dávalos, L. M., P. M. Velazco, O. M. Warsi, P. D. Smits, and N. B. Simmons. 2014. Integrating incomplete fossils by isolating conflicting signal in saturated and non-independent morphological characters. Systematic Biology 63:582–600.

Degnan, J. H., and N. A. Rosenberg. 2009. Gene tree discordance, phylogenetic inference and the multispecies coalescent. Trends in Ecology & Evolution 24:332–340.

Denzinger, A., and H. U. Schnitzler. 2013. Bat guilds, a concept to classify the highly diverse foraging and echolocation behaviors of microchiropteran bats. Frontiers in Physiology 4:164.

De Oliveira, L. Q., R. Marciente, W. E. Magnusson, and P. E. D. Bobrowiec. 2015. Activity of the insectivorous bat *Pteronotus parnellii* relative to insect resources and vegetation structure. Journal of Mammalogy 96:1036–1044.

Emrich, M. A., E. L. Clare, W. O. Symondson, S. E. Koenig, and M. B. Fenton. 2014. Resource partitioning by insectivorous bats in Jamaica. Molecular Ecology 23:3648–3656.

Feder, J. L., S. M. Flaxman, S. P. Egan, A. A. Comeault, and P. Nosil. 2013. Geographic mode of speciation and genomic divergence. Annual Review of Ecology, Evolution, and Systematics 44:73–97.

Ferreri, M., W. Qu, and B. Han. 2011. Phylogenetic networks: a tool to display character conflict and demographic history. African Journal of Biotechnology 10:12799–12803.

Fu, Y. X. 1997. Statistical tests of neutrality of mutations against population growth, hitchhiking and background selection. Genetics 147:915–925.

Gray, J. E. 1838. A revision of the genera of bats (Vespertilionidae), and the description of some new genera and species. Magazine of Zoology and Botany 2:483–505.

Gray, J. E. 1839. Description of some Mammalia discovered in Cuba by W. S. MacLeay, Esq. Annals of Natural History 4:1–7.

Gray, J. E. 1843. [Untitled letter addressed to the Curator]. Proceedings of the Zoological Society of London 1843:50.

Gundlach, J. 1840. Beschreibung von vier auf Cuba gefangnen Fledermauden. Arch Naturgesch 6:356–358.

Gutiérrez, E. E., and J. Molinari. 2008. Morphometrics and taxonomy of bats of the genus *Pteronotus* (subgenus *Phyllodia*) in Venezuela. Journal of Mammalogy 89:292–305.

Herd, R. M. 1983. *Pteronotus parnellii*. Mammalian Species 209:1–5.

Honacki, J. H., K. E. Kinman, and J. W. Koeppl. 1982. Mammal species of the world: a taxonomic and geographic reference. Allen Press and the Association of Systematics Collections, Lawrence, Kansas.

Husson, A. M. 1962. The bats of Suriname. Zoologische Verhandelingen 58:1–278.

Jones, G. 1997. Acoustic signals and speciation: the roles of natural and sexual selection in the evolution of cryptic species. Advances in the Study of Behavior 26:317–354.

Jones, G., and K. E. Barlow. 2004. Cryptic species of echolocating bats. Pp. 345–349 in Echolocation in bats and dolphins (J. A. Thomas, C. F. Moss, and M. Vater, eds.). University of Chicago Press, Chicago, Illinois.

Kingston, T., M. C. Lara, G. Jones, Z. Akbar, T. H. Kunz, and C. J. Schneider. 2001. Acoustic divergence in two cryptic *Hipposideros* species: a role for social selection? Proceedings of the Royal Society of London B: Biological Sciences 268:1381–1386.

Klekca, R. W. 1980. Discriminant analysis. Sage University Paper Series Quantitative Applications in the Social Sciences. Sage Publications, Beverly Hills, California.

Lewis-Oritt, N., C. A. Porter, and R. J. Baker. 2001. Molecular systematics of the family Mormoopidae (Chiroptera) based on cytchrome b and recombination activating gene 2 sequences. Molecular Phylogenetics and Evolution 20:26–436.

Librado, P., and J. Rozas. 2009. Dnasp v5: a software for comprehensive analysis of DNA polymorphism data. Bioinformatics (Oxford, England) 25:1451–1452.

López-Baucells, A., R. Rocha, P. E. D. Bobrowiec, E. Bernard, J. Palmeirim, and C. Meyer. 2016. Field guide to Amazonian bats. Editora INPA, Manaus, Brazil.

López-Baucells, A., L. Torrent, R. Rocha, A. C. Pavan, P. E. D. Bobrowiec, and C. F. J. Meyer. 2017. Geographical variation in the high-duty cycle echolocation of the cryptic common mustached bat *Pteronotus* cf. *rubiginosus* (Mormoopidae). Bioacoustics 1–17.

Losos, J. B. 2000. Ecological character displacement and the study of adaptation. Proceedings of the National Academy of Sciences 97:5693–5695.

Mancina, C. A. 2005. *Pteronotus macleayii*. Mammalian Species 778:1–3.

Mancina, C. A., L. García-Rivera, and B. W. Miller. 2012. Wing morphology, echolocation, and resource partitioning in syntopic Cuban mormoopid bats. Journal of Mammalogy 93:1308–1317.

Nei, M. 1987. Molecular evolutionary genetics. Columbia University Press, New York.

Nogueira, M. R., I. P. Lima, A. L. Peracchi, and N. B. Simmons. 2012. New genus and species of nectar-feeding bat from the Atlantic Forest of Southeastern Brazil (Chiroptera: Phyllostomidae: Glossophaginae). American Museum Novitates 3747:1–30.

Patton, J. L., and A. L. Gardner. 2008. Family mormoopidae. Pp. 376–384 in Mammals of South America. Volume 1. Marsupials, xenarthrans, shrews, and bats (A. L. Gardner, ed.). University of Chicago Press, Chicago, Illinois.

Pavan, A. C., and G. Marroig. 2016. Integrating multiple evidences in taxonomy: species diversity and phylogeny of mustached bats (Mormoopidae: *Pteronotus*). Molecular Phylogenetics and Evolution 103:184–198.

Pavan, A. C., and G. Marroig. 2017. Timing and patterns of diversification in the Neotropical bat genus *Pteronotus* (Mormoopidae). Molecular Phylogenetics and Evolution 108:61–69.

Petit, R. J., and L. Excoffier. 2009. Gene flow and species delimitation. Trends in Ecology & Evolution 24:386–393.

Pfennig, K. S., and D. W. Pfennig. 2009. Character displacement: ecological and reproductive responses to a common evolutionary problem. The Quarterly Review of Biology 84:253–276.

Pfennig, K. S., and D. W. Pfennig. 2010. Character displacement and the origins of diversity. The American Naturalist 176 (Suppl. 1):S26–S44.

Ponzio, R. 2017. Efeitos da insularização sobre a assembléia de morcegos insetívoros aéreos na Hidrelétrica de Balbina, Amazônia Central. M.S. thesis, Instituto Nacional de Pesquisas da Amazônia, Manaus, Brazil.

R Development Core Team. 2013. R: a language and environment for statistical computing. R Foundation for Statistical Computing, Vienna, Austria.

Rehn, J. A. G. 1904. A study of the Mammalian genus *Chilonycteris*. Proceedings of the Academy of Natural Sciences of Philadelphia 56:181–207.

Rocha, P. A., J. A. Feijó, J. S. Mikalauskas, and S. F. Ferrari. 2011. First records of mormoopid bats (Chiroptera, Mormoopidae) from the Brazilian Atlantic Forest. Mammalia 75:295–299.

Rolfe, A. K., and A. Kurta. 2012. Diet of mormoopid bats on the Caribbean island of Puerto Rico. Acta Chiropterologica 14:369–377.

Santana, S. E., and S. E. Lofgren. 2013. Does nasal echolocation influence the modularity of the mammal skull? Journal of Evolutionary Biology 26:2520–2526.

Schluter, D., and J. D. McPhail. 1992. Ecological character displacement and speciation in sticklebacks. The American Naturalist 140:85–108.

Schnitzler, H. U., and A. Denzinger. 2011. Auditory fovea and Doppler shift compensation: adaptations for flutter detection in echolocating bats using CF-FM signals. Journal of Comparative Physiology. A, Neuroethology, Sensory, Neural, and Behavioral Physiology 197:541–559.

Simmons, N. B., and T. M. Conway. 2001. Phylogenetic relationships of mormoopid bats (Chiroptera: Mormoopidae) based on morphological data. Bulletin of the American Museum of Natural History 258:1–97.

Smith, J. D. 1972. Systematics of the chiropteran family Mormoopidae. Miscellaneous Publication, Museum of Natural History, University of Kansas 56:1–132.

Tajima, F. 1989. Statistical method for testing the neutral mutation hypothesis by DNA polymorphism. Genetics 123:585–595.

Tamura, K., G. Stecher, D. Peterson, A. Filipski, and S. Kumar. 2013. MEGA6: molecular evolutionary genetics analysis version 6.0. Molecular Biology and Evolution 30:2725–2729.

Thoisy, B. D., et al. 2014. Cryptic diversity in common mustached bats *Pteronotus* cf. *parnellii* (Mormoopidae) in French Guiana and Brazilian Amapa. Acta Chiropterologica 16:1–13.

Velazco, P., and B. Patterson. 2014. Two new species of yellow-shouldered bats, genus *Sturnira* Gray, 1842 (Chiroptera, Phyllostomidae) from Costa Rica, Panama and western Ecuador. ZooKeys 402:43–66.

Wagner, J. A. 1843. Diagnosen neuer Arten brasilischer Handflungler. Arch Naturgesch 9:365–368.

Wakeley, J. 2004. Inferences about the structure and history of populations: coalescents and intraspecific phylogeography. Pp. 193–215 in The evolution of population biology (R. S. Singh and M. K. Uyenoyama, eds.). Cambridge University Press, Cambridge, United Kingdom.

Submitted 5 January 2018. Accepted 29 April 2018.

Associate Editor was Ricardo Moratelli.

Appendix I

Specimens included in the molecular, morphometric, and acoustic datasets.

A = acoustic dataset; *COI* = sequence of the cytochrome oxidase I gene; FN = field number; GN = GenBank number; M = morphometric dataset; S = sex; VN = voucher number.

AMNH = American Museum of Natural History; IEPA = Instituto de Pesquisas Científicas e Tecnológicas do Estado do Amapá; INPA = Instituto Nacional de Pesquisas da Amazônia; LM-ESALQ = Laboratorio de Mamíferos-ESALQ; MHNG = Musée d'Histoire Naturelle – Genève; MPEG = Museu Paraense Emílio Goeldi; MZUSP = Museu de Zoologia da Universidade de São Paulo; ROM = Royal Ontario Museum; TTU = Texas Tech University; UEMA = Universidade Estadual do Maranhão; UFMG = Universidade Federal de Minas Gerais.

BRA-AM = Brazilian state of Amazonas; BRA-AP = Brazilian state of Amapá; BRA-MT = Brazilian state of Mato Grosso; BRA-PA = Brazilian state of Pará ; BRA-PI = Brazilian state of Piauí ; BRA-RO = Brazilian state of Rondônia ; FGU = French Guiana; GUY = Guyana; SUR = Suriname.

X = type of data included for the specimen.

VN		FN	S	Species	Locality	Country	Population	M	A	*COI*	GN
MZUSP	35514	RB06	M	*Pteronotus rubiginosus*	Ribeirãozinho, Mato Grosso	Brazil	BRA-MT	X		X	KX590144
MZUSP	35515	RB09	F	*P. rubiginosus*	Ribeirãozinho, Mato Grosso	Brazil	BRA-MT	X		X	KX590145
MZUSP	35151	AC1334	F	*P. rubiginosus*	Cuiabá, Mato Grosso	Brazil	BRA-MT	X			
MZUSP	35152	AC1362	M	*P. rubiginosus*	Cuiabá, Mato Grosso	Brazil	BRA-MT	X		X	KF636799
MZUSP	35513	AC1396	F	*P. rubiginosus*	Rondonópolis, Mato Grosso	Brazil	BRA-MT	X		X	KX590131
MZUSP	35147	FM43	F	*P. rubiginosus*	Jangada, Mato Grosso	Brazil	BRA-MT	X		X	KX590153
MZUSP	35148	FM45	F	*P. rubiginosus*	Jangada, Mato Grosso	Brazil	BRA-MT	X		X	KX590154
MZUSP	35149	FM47	F	*P. rubiginosus*	Jangada, Mato Grosso	Brazil	BRA-MT	X		X	KX590155
MZUSP	35150	FM52	M	*P. rubiginosus*	Jangada, Mato Grosso	Brazil	BRA-MT	X		X	KX590157
MZUSP	35153	MN70 14	M	*P. rubiginosus*	São Vicente, Mato Grosso	Brazil	BRA-MT	X		X	KX590159
MZUSP	35154	MN70 30	F	*P. rubiginosus*	São Vicente, Mato Grosso	Brazil	BRA-MT	X		X	KX590160
MZUSP	35155	MN70 42	F	*P. rubiginosus*	São Vicente, Mato Grosso	Brazil	BRA-MT	X		X	KX590162
MPEG	41678	ACP32	F	*P. alitonus*	Itaituba, Pará	Brazil	BRA-AM	X		X	KX590146
MZUSP	35503	ACP135	F	*P. alitonus*	Itaituba, Pará	Brazil	BRA-AM	X		X	KX590147
MZUSP	35504	ACP158	F	*P. alitonus*	Itaituba, Pará	Brazil	BRA-AM	X		X	KX590148
MZUSP	35505	ACP173	F	*P. alitonus*	Itaituba, Pará	Brazil	BRA-AM	X		X	KX590149
MZUSP	35506	AC1118	F	*P. rubiginosus*	FLONA Tapirapé-Aquiri, Marabá, Pará	Brazil	BRA-PA	X		X	KX590129
MZUSP	35508	AC1524	M	*P. rubiginosus*	FLONA Tapirapé-Aquiri, Marabá, Pará	Brazil	BRA-PA	X		X	KX590134
MZUSP	35510	AC1023	F	*P. rubiginosus*	FLONA Tapirapé-Aquiri, Marabá, Pará	Brazil	BRA-PA	X			
MPEG	38828	AC254	F	*P. rubiginosus*	FLONA Tapirapé-Aquiri, Marabá, Pará	Brazil	BRA-PA	X			
MPEG	38809	AC377	F	*P. rubiginosus*	FLONA Tapirapé-Aquiri, Marabá, Pará	Brazil	BRA-PA	X			
MZUSP	35512	AC670	M	*P. rubiginosus*	FLONA Tapirapé-Aquiri, Marabá, Pará	Brazil	BRA-PA	X			
MZUSP	35509	AC1911	F	*P. rubiginosus*	FLONA Tapirapé-Aquiri, Marabá, Pará	Brazil	BRA-PA	X		X	KX590139
MZUSP		AC1046	F	*P. rubiginosus*	FLONA Tapirapé-Aquiri, Marabá, Pará	Brazil	BRA-PA			X	KX590127
MZUSP		AC939	M	*P. rubiginosus*	Tesouro, Mato Grosso	Brazil	BRA-MT			X	KX590143
MZUSP		MN70_07	F	*P. rubiginosus*	São Vicente, Mato Grosso	Brazil	BRA-MT			X	KX590158
MZUSP		MN70_37	F	*P. rubiginosus*	São Vicente, Mato Grosso	Brazil	BRA-MT			X	KX590161
MZUSP	35702	EG153	M	*P. rubiginosus*	Serra das Araras, Mato Grosso	Brazil	BRA-MT	X			
MZUSP	35703	EG183	F	*P. rubiginosus*	Serra das Araras, Mato Grosso	Brazil	BRA-MT	X			
MZUSP	35704	EG191	U	*P. rubiginosus*	Serra das Araras, Mato Grosso	Brazil	BRA-MT	X			
MZUSP	35705	EG206	M	*P. rubiginosus*	Serra das Araras, Mato Grosso	Brazil	BRA-MT	X			
MZUSP	35706	EG235	M	*P. rubiginosus*	Serra das Araras, Mato Grosso	Brazil	BRA-MT	X			
MZUSP	35707	EG246	M	*P. rubiginosus*	Serra das Araras, Mato Grosso	Brazil	BRA-MT	X			
MZUSP	29504		M	*P. rubiginosus*	Pontes Larcerda, Mato Grosso	Brazil	BRA-MT	X			
MZUSP	35701	N2012	M	*P. rubiginosus*	Vilhena, Rondônia	Brazil	BRA-RO	X		X	KX590163
MZUSP	35699	AC1817	F	*P. rubiginosus*	Vilhena, Rondônia	Brazil	BRA-RO	X		X	KX590135
MZUSP	35700	AC1820	M	*P. rubiginosus*	Vilhena, Rondônia	Brazil	BRA-RO	X		X	KX590136
MZUSP	35516	CCA1840	F	*P. rubiginosus*	Rio Madeira, UHE Jirau, Porto Velho, Rondônia	Brazil	BRA-RO	X			
MZUSP	35517	CCA1899	M	*P. rubiginosus*	Rio Madeira, UHE Jirau, Porto Velho, Rondônia	Brazil	BRA-RO	X			
MZUSP	35511	CCA919	M	*P. rubiginosus*	Rio Madeira, UHE Jirau, Porto Velho, Rondônia	Brazil	BRA-RO	X			
MZUSP		CCA1226	U	*P. rubiginosus*	Rio Madeira, UHE Jirau, Porto Velho, Rondônia	Brazil	BRA-RO			X	KX590150
MZUSP		CCA1267	U	*P. rubiginosus*	Rio Madeira, UHE Jirau, Porto Velho, Rondônia	Brazil	BRA-RO			X	KX590151
MZUSP		CCA1324	U	*P. rubiginosus*	Rio Madeira, UHE Jirau, Porto Velho, Rondônia	Brazil	BRA-RO			X	KX590152

VN		FN	S	Species	Locality	Country	Population	M	A	*COI*	GN
MZUSP		QTPC13	U	*P. rubiginosus*	UHE Teles Pires, Paranaíta, Mato Grosso	Brazil	BRA-MT			X	KX590164
MZUSP		QTPC18	U	*P. rubiginosus*	UHE Teles Pires, Paranaíta, Mato Grosso	Brazil	BRA-MT			X	KX590165
MZUSP	30035		M	*P. rubiginosus*	E.E. Uruçui-Una, Bom Jesus, Piauí	Brazil	BRA-PI	X			
MZUSP	30120		U	*P. rubiginosus*	E.E. Uruçui-Una, Bom Jesus, Piauí	Brazil	BRA-PI	X			
MZUSP	30142		U	*P. rubiginosus*	E.E. Uruçui-Una, Bom Jesus, Piauí	Brazil	BRA-PI	X			
MZUSP	30155		F	*P. rubiginosus*	E.E. Uruçui-Una, Bom Jesus, Piauí	Brazil	BRA-PI	X			
MZUSP	30210		F	*P. rubiginosus*	E.E. Uruçui-Una, Bom Jesus, Piauí	Brazil	BRA-PI	X			
MZUSP	35518	GA0656	F	*P. alitonus*	Amaila Falls, Potaro-Siparuni	Guyana	GUY	X			
MZUSP	35519	GA0658	M	*P. rubiginosus*	Amaila Falls, Potaro-Siparuni	Guyana	GUY	X		X	MH017827
MZUSP	35520	GA0559	M	*P. alitonus*	Amaila Falls, Potaro-Siparuni	Guyana	GUY	X		X	MH017828
MZUSP	35521	GA0625	M	*P. alitonus*	Amaila Falls, Potaro-Siparuni	Guyana	GUY	X			MH017827
MZUSP	35522	GA0560	F	*P. alitonus*	Amaila Falls, Potaro-Siparuni	Guyana	GUY	X			
MZUSP	35523	GA0637	F	*P. alitonus*	Amaila Falls, Potaro-Siparuni	Guyana	GUY	X		X	MH017829
MZUSP	35525	GA0613	M	*P. alitonus*	Amaila Falls, Potaro-Siparuni	Guyana	GUY			X	MH017830
MZUSP	35527	V7Q01	F	*P. alitonus*	Amaila Falls, Potaro-Siparuni	Guyana	GUY	X			
MZUSP	35528	V7Q06	F	*P. rubiginosus*	Amaila Falls, Potaro-Siparuni	Guyana	GUY			X	MH017831
MZUSP	35529	V7Q08	F	*P. alitonus*	Amaila Falls, Potaro-Siparuni	Guyana	GUY	X			
LM-ESALQ		ABX58	F	*P. rubiginosus*	Paca-Mirim, margem direita Rio Abacaxis, margem direita Rio Madeira, Amazonas	Brazil	BRA-AM	X		X	MH017832
LM-ESALQ		ABX60	F	*P. rubiginosus*	Paca-Mirim, margem direita Rio Abacaxis, margem direita Rio Madeira, Amazonas	Brazil	BRA-AM			X	MH017833
UFMG		BOC541	M	*P. rubiginosus*	Canaã dos Carajás, Pará	Brazil	BRA-PA			X	KX590311
UFMG		BOC548	M	*P. rubiginosus*	Canaã dos Carajás, Pará	Brazil	BRA-PA			X	KX590314
UFMG		BOC575	M	*P. rubiginosus*	Canaã dos Carajás, Pará	Brazil	BRA-PA			X	KX590317
UFMG		BOC602	M	*P. rubiginosus*	Canaã dos Carajás, Pará	Brazil	BRA-PA			X	KX590318
UFMG		BOC652	F	*P. rubiginosus*	Canaã dos Carajás, Pará	Brazil	BRA-PA			X	KX590319
UFMG		BOC655	M	*P. rubiginosus*	Canaã dos Carajás, Pará	Brazil	BRA-PA			X	KX590320
UFMG		VCT1072	M	*P. rubiginosus*	Parauapebas/Canaã dos Carajás, Pará	Brazil	BRA-PA			X	KX590323
UFMG		VCT1103	M	*P. rubiginosus*	Parauapebas/Canaã dos Carajás, Pará	Brazil	BRA-PA			X	KX590324
UFMG		VCT1135	F	*P. rubiginosus*	Parauapebas/Canaã dos Carajás, Pará	Brazil	BRA-PA			X	KX590325
UFMG		VCT1741	F	*P. rubiginosus*	FLONA Carajás, Canaã dos Carajás, Pará	Brazil	BRA-PA			X	KX590328
UFMG		VCT1773	F	*P. rubiginosus*	FLONA Carajás, Canaã dos Carajás, Pará	Brazil	BRA-PA			X	KX590331
UFMG		VCT1775	M	*P. rubiginosus*	FLONA Carajás, Canaã dos Carajás, Pará	Brazil	BRA-PA			X	KX590332
UFMG		VCT1869	M	*P. rubiginosus*	FLONA Carajás, Canaã dos Carajás, Pará	Brazil	BRA-PA			X	KX590334
UFMG		VCT1871	M	*P. rubiginosus*	FLONA Carajás, Canaã dos Carajás, Pará	Brazil	BRA-PA			X	KX590335
UFMG		VCT1873	M	*P. rubiginosus*	FLONA Carajás, Canaã dos Carajás, Pará	Brazil	BRA-PA			X	KX590336
UFMG		VCT2824	F	*P. rubiginosus*	FLONA Carajás, Canaã dos Carajás, Pará	Brazil	BRA-PA			X	KX590342
UFMG		VCT3048	F	*P. rubiginosus*	FLONA Carajás, Canaã dos Carajás, Pará	Brazil	BRA-PA			X	KX590343
UFMG		VCT3055	M	*P. rubiginosus*	FLONA Carajás, Canaã dos Carajás, Pará	Brazil	BRA-PA			X	KX590344
UFMG		VCT3846	M	*P. rubiginosus*	Tapa Oeste, Xinguara, Pará	Brazil	BRA-PA			X	KX590347
UFMG		VCT3880	F	*P. rubiginosus*	Serra do Tapa, Xinguara, Pará	Brazil	BRA-PA			X	KX590348
UFMG		VCT4953	F	*P. rubiginosus*	FLONA Carajás, Canaã dos Carajás, Pará	Brazil	BRA-PA			X	KX590349
UFMG		VCT5139	F	*P. rubiginosus*	FLONA Carajás, Canaã dos Carajás, Pará	Brazil	BRA-PA			X	KX590351
UFMG		VCT6099	F	*P. rubiginosus*	Marabá, Pará	Brazil	BRA-PA			X	KX590352
UFMG		VCT6224	M	*P. rubiginosus*	FLONA Carajás N5, Parauapebas, Pará	Brazil	BRA-PA			X	KX590353
UFMG		VCT6228	M	*P. rubiginosus*	FLONA Carajás N5, Parauapebas, Pará	Brazil	BRA-PA			X	KX590355
UFMG		VCT6255	M	*P. rubiginosus*	FLONA Carajás N5, Parauapebas, Pará	Brazil	BRA-PA			X	KX590361
UFMG		VCT6370	F	*P. rubiginosus*	FLONA Carajás N5, Parauapebas, Pará	Brazil	BRA-PA			X	KX590362
UFMG		VCT6376	M	*P. rubiginosus*	FLONA Carajás N5, Parauapebas, Pará	Brazil	BRA-PA			X	KX590363

VN		FN	S	Species	Locality	Country	Population	M	A	*COI*	GN
UFMG		ARI03	M	*P. rubiginosus*	Aripuanã, Mato Grosso	Brazil	BRA-MT			X	KX590276
UFMG		ARI08	F	*P. rubiginosus*	Aripuanã, Mato Grosso	Brazil	BRA-MT			X	KX590277
UFMG		ARI16	F	*P. rubiginosus*	Aripuanã, Mato Grosso	Brazil	BRA-MT			X	KX590278
UFMG		ARI33	M	*P. rubiginosus*	Aripuanã, Mato Grosso	Brazil	BRA-MT			X	KX590279
UFMG		TG22	M	*P. rubiginosus*	Teotônio, Porto Velho, Rondônia	Brazil	BRA-RO			X	KX590126
UEMA		U.62	F	*P. rubiginosus*	Uruçuí, Piauí	Brazil	BRA-PI			X	KX590281
UEMA		91.3	M	*P. rubiginosus*	Amarante, Maranhão	Brazil	BRA-PI			X	KX590282
UEMA		92.1	U	*P. rubiginosus*	Parnarama, Maranhão	Brazil	BRA-PI			X	KX590280
IEPA	380	MAP276	M	*P. alitonus*	Rio Cupixi, RDS Iratapuru, Pedra Branca do Amapari, Amapá	Brazil	BRA-AP	X			
IEPA	415	MAP311	F	*P. alitonus*	Rio Cupixi, RDS Iratapuru, Pedra Branca do Amapari, Amapá	Brazil	BRA-AP	X		X	KX590104
IEPA	417	MAP313	M	*P. alitonus*	Rio Cupixi, RDS Iratapuru, Pedra Branca do Amapari, Amapá	Brazil	BRA-AP	X		X	KX590105
IEPA	418	MAP314	M	*P. rubiginosus*	Rio Cupixi, RDS Iratapuru, Pedra Branca do Amapari, Amapá	Brazil	BRA-AP	X		X	KX590106
IEPA	428	MAP324	M	*P. rubiginosus*	Rio Cupixi, RDS Iratapuru, Pedra Branca do Amapari, Amapá	Brazil	BRA-AP	X		X	KX590107
IEPA	456	MAP336	F	*P. alitonus*	P.N.Tumucumaque, Rio Anoteie, Oiapoque, Amapá	Brazil	BRA-AP	X		X	KX590108
IEPA	476	MAP358	F	*P. rubiginosus*	P.N.Tumucumaque, Rio Anoteie, Oiapoque, Amapá	Brazil	BRA-AP	X		X	KX590109
IEPA	525	MAP377	F	*P. rubiginosus*	P.N.Tumucumaque, Rio Mutum, Calçoene, Amapá	Brazil	BRA-AP	X		X	KX590110
IEPA	533	MAP385	M	*P. rubiginosus*	P.N.Tumucumaque, Rio Mutum, Calçoene, Amapá	Brazil	BRA-AP	X		X	KX590111
IEPA	554	MAP406	F	*P. rubiginosus*	P.N.Tumucumaque, Rio Mutum, Calçoene, Amapá	Brazil	BRA-AP	X		X	KF636800
IEPA	722	MAP437	M	*P. rubiginosus*	área de Cerrado, Fazenda Aricari/BR156, km 147, Tartarugalzinho, Amapá	Brazil	BRA-AP	X		X	KX590112
IEPA	748	MAP463	F	*P. rubiginosus*	área de Cerrado, Fazenda Aricari/BR156, km 147, Tartarugalzinho, Amapá	Brazil	BRA-AP	X		X	KX590113
IEPA	758	MAP473	F	*P. rubiginosus*	área de Cerrado, Fazenda Aricari/BR156, km 147, Tartarugalzinho, Amapá	Brazil	BRA-AP	X		X	KX590114
IEPA	760	MAP475	F	*P. rubiginosus*	área de Cerrado, Fazenda Aricari/BR156, km 147, Tartarugalzinho, Amapá	Brazil	BRA-AP	X		X	KX590115
IEPA	1833	UHSA22	F	*P. alitonus*	Rio Jari, Laranjal do Jari, Amapá	Brazil	BRA-AP	X		X	KX590116
IEPA	1843	UHSA32	M	*P. alitonus*	Rio Jari, Laranjal do Jari, Amapá	Brazil	BRA-AP	X		X	KF636815
IEPA	1847	UHSA36	F	*P. alitonus*	Rio Jari, Laranjal do Jari, Amapá	Brazil	BRA-AP	X		X	KX590117
IEPA	1853	UHSA42	F	*P. alitonus*	Rio Jari, Laranjal do Jari, Amapá	Brazil	BRA-AP	X		X	KX590118
IEPA	1893	UHSA15	F	*P. alitonus*	Rio Jari, Laranjal do Jari, Amapá	Brazil	BRA-AP	X		X	KX590119
INPA	6941	PP01	M	*P. rubiginosus*	PDBFF, Manaus, Amazonas	Brazil	BRA-AM	X	X	X	MH017834
INPA	6942	PP02	M	*P. alitonus*	PDBFF, Manaus, Amazonas	Brazil	BRA-AM	X	X	X	MH017835
INPA	6943	PP03	F	*P. rubiginosus*	PDBFF, Manaus, Amazonas	Brazil	BRA-AM	X	X	X	MF547497
INPA	6944	PP05	M	*P. rubiginosus*	PDBFF, Manaus, Amazonas	Brazil	BRA-AM	X	X		
INPA	6945	PP11	F	*P. alitonus*	PDBFF, Manaus, Amazonas	Brazil	BRA-AM	X	X	X	MF547493
INPA	6946	PP14	F	*P. rubiginosus*	PDBFF, Manaus, Amazonas	Brazil	BRA-AM	X	X	X	MF547498
INPA	6947	PP16	M	*P. alitonus*	PDBFF, Manaus, Amazonas	Brazil	BRA-AM	X	X	X	MH017836
INPA	6948	PP21	F	*P. alitonus*	PDBFF, Manaus, Amazonas	Brazil	BRA-AM	X	X	X	MF547495
INPA	6949	PP22	F	*P. alitonus*	PDBFF, Manaus, Amazonas	Brazil	BRA-AM	X	X	X	MF547496

VN		FN	S	Species	Locality	Country	Population	M	A	*COI*	GN
INPA	6950	PP24	M	*P. alitonus*	PDBFF, Manaus, Amazonas	Brazil	BRA-AM	X	X	X	MF547494
INPA	6951	PP25	F	*P. rubiginosus*	PDBFF, Manaus, Amazonas	Brazil	BRA-AM	X	X	X	MF547499
INPA	6952	PP26	F	*P. alitonus*	PDBFF, Manaus, Amazonas	Brazil	BRA-AM	X	X	X	MH017837
INPA	6953	PP30	F	*P. rubiginosus*	PDBFF, Manaus, Amazonas	Brazil	BRA-AM		X	X	MF547500
INPA	6954	PP31	F	*P. alitonus*	PDBFF, Manaus, Amazonas	Brazil	BRA-AM	X	X	X	MF547501
INPA	6955	PP34	F	*P. rubiginosus*	PDBFF, Manaus, Amazonas	Brazil	BRA-AM	X	X	X	MF547502
INPA	6085	IC12	F	*P. rubiginosus*	Porto Velho, Rondônia	Brazil	BRA-RO			X	KX590120
INPA	6100	IF09	M	*P. rubiginosus*	Porto Velho, Rondônia	Brazil	BRA-RO			X	KX590121
INPA	6120	JCDA08	M	*P. rubiginosus*	Porto Velho, Rondônia	Brazil	BRA-RO			X	KX590122
INPA	6129	JCDD16	M	*P. rubiginosus*	Porto Velho, Rondônia	Brazil	BRA-RO			X	KX590123
INPA	6162	JRDB13	F	*P. rubiginosus*	Porto Velho, Rondônia	Brazil	BRA-RO			X	KX590124
INPA	6172	JRDD06	M	*P. rubiginosus*	Porto Velho, Rondônia	Brazil	BRA-RO			X	KX590125
AMNH	267283	NBS494	F	*P. rubiginosus*	Paracou	French Guiana	FGU	X			
AMNH	267286	NBS524	M	*P. rubiginosus*	Paracou	French Guiana	FGU	X			
AMNH	269115	NBS809	M	*P. rubiginosus*	Paracou	French Guiana	FGU	X		X	KX590080
AMNH	267851	NBS904	F	*P. alitonus*	Paracou	French Guiana	FGU	X		X	KX590081
AMNH	267288	NBS549	M	*P. rubiginosus*	Paracou	French Guiana	FGU	X			
AMNH	267284	NBS543	M	*P. rubiginosus*	Paracou	French Guiana	FGU	X			
AMNH	267285	NBS521	M	*P. rubiginosus*	Paracou	French Guiana	FGU	X			
AMNH	267406	SES237	F	*P. alitonus*	Paracou	French Guiana	FGU	X			
AMNH	267405	SES209	F	*P. alitonus*	Paracou	French Guiana	FGU			X	KX590086
ROM	100391	F34632	F	*P. rubiginosus*	Mango Landing, Corentyne River, East Berbice-Corentyne	Guyana	GUY	X		X	JF448242
ROM	100397	F34638	F	*P. rubiginosus*	Mango Landing, Corentyne River, East Berbice-Corentyne	Guyana	GUY	X		X	JF448220
ROM	100427	F34668	F	*P. alitonus*	Mango Landing, Corentyne River, East Berbice-Corentyne	Guyana	GUY	X		X	JF448247
ROM	97957	FN33458	M	*P. rubiginosus*	Karanambo, Upper Takutu-Upper Essequibo	Guyana	GUY	X		X	JF448258
ROM	98128	FN31130	F	*P. alitonus*	Kurupukari, East Bank, Essequibo River, Upper Demerara-Berbice	Guyana	GUY	X		X	JF448217
ROM	97963	FN33464	M	*P. rubiginosus*	Annai, Upper Takutu-Upper Essequibo	Guyana	GUY	X		X	JF448259
ROM	97964	FN33465	M	*P. rubiginosus*	Annai, Upper Takutu-Upper Essequibo	Guyana	GUY	X		X	JF448260
ROM	98127	FN31129	F	*P. rubiginosus*	Kurupukari, East Bank, Essequibo River, Upper Demerara-Berbice	Guyana	GUY	X		X	JF448216
ROM	102991	F36454	M	*P. rubiginosus*	5 km SE Surama, Upper Takutu-Upper Essequibo	Guyana	GUY	X		X	JF448393
ROM	103375	F36838	F	*P. rubiginosus*	Tropenbos, 20 km SSE Mabura Hill, Upper Demerara-Berbice	Guyana	GUY	X		X	JF448377
ROM	104705	F38296	F	*P. alitonus*	Iwokrama Reserve, 25 km SSW Kurupukari, Potaro-Siparuni	Guyana	GUY	X		X	JF448408
ROM	106575	F38572	F	*P. rubiginosus*	Chodikar River, 55 km SW Gunn's Strip, Upper Takutu-Upper Essequibo	Guyana	GUY	X		X	JF448290
ROM	106585	F38582	F	*P. alitonus*	Chodikar River, 55 km SW Gunn's Strip, Upper Takutu-Upper Essequibo	Guyana	GUY	X		X	JF448291
ROM	106776	F38773	F	*P. alitonus*	Gunn's Strip, Upper Takutu-Upper Essequibo	Guyana	GUY	X		X	JF448295
ROM	102973	F36436	M	*P. alitonus*	5 km SE Surama, Upper Takutu-Upper Essequibo	Guyana	GUY	X		X	JF448391

VN		FN	S	Species	Locality	Country	Population	M	A	*COI*	GN
ROM	103374	F36837	F	*P. alitonus*	Tropenbos, 20 km SSE Mabura Hill, Upper Demerara-Berbice	Guyana	GUY	X		X	JF448376
ROM	103420	F36883	M	*P. rubiginosus*	Tropenbos, 20 km SSE Mabura Hill, Upper Demerara-Berbice	Guyana	GUY	X		X	JF448379
ROM	106659	F38656	M	*P. alitonus*	Kamoa River, 50 km SWW Gunn's Strip, Upper Takutu-Upper Essequibo	Guyana	GUY	X		X	JF448292
ROM	120275	F53063	F	*P. alitonus*	Iconja Landing, Sipaliwini River, Sipaliwini	Suriname	SUR	X		X	HQ545477
ROM	120294	F53082	M	*P. alitonus*	Iconja Landing, Sipaliwini River, Sipaliwini	Suriname	SUR	X		X	HQ919657
ROM	120589	F53299	F	*P. alitonus*	Kutari River Camp, Sipaliwini	Suriname	SUR	X		X	JQ601193
ROM	120631	F53341	M	*P. alitonus*	Sipaliwini River Camp, Sipaliwini	Suriname	SUR	X		X	JQ601223
ROM	120645	F53355	F	*P. alitonus*	Sipaliwini River Camp, Sipaliwini	Suriname	SUR	X		X	JQ601237
ROM	120408	F53196	F	*P. rubiginosus*	Sipaliwini Village, Sipaliwini	Suriname	SUR	X		X	HQ919758
ROM	117576	F54897	F	*P. alitonus*	Blanche Marie Vallen, Sipaliwini	Suriname	SUR	X		X	EU096919
ROM	117608	F54929	M	*P. rubiginosus*	Blanche Marie Vallen, Sipaliwini	Suriname	SUR	X		X	EU096918
ROM	117654	F54975	F	*P. rubiginosus*	Blanche Marie Vallen, Sipaliwini	Suriname	SUR	X		X	EU096924
ROM	117282	F54603	M	*P. rubiginosus*	Bakhuis, Transect 13, Sipaliwini	Suriname	SUR	X		X	EU096906
ROM	117338	F54659	F	*P. rubiginosus*	Bakhuis, Transect 14, Sipaliwini	Suriname	SUR	X		X	EU096908
ROM	117545	F54866	F	*P. alitonus*	Bakhuis, Area 8 Recon Fly Camp, Sipaliwini	Suriname	SUR	X		X	EU096917
ROM	113978	F41053	M	*P. rubiginosus*	Brownsberg Nature Park, jeep trail, Brokopondo	Suriname	SUR			X	JF448284
ROM	115699	F51063	F	*P. alitonus*	Iwokrama field Station, Potaro-Siparuni	Guyana	GUY			X	JF448175
MHNG	1972_050	V-2637	U	*P. rubiginosus*	Reserve Trésor (entre Kaw et Roura)	French Guiana	FGU	X	X		
MHNG	1972_051	V-2638	U	*P. alitonus*	Kaw: Grotte Mathilde	French Guiana	FGU	X	X		
MHNG	1972_052	V-2639	U	*P. alitonus*	Reserve Trésor (entre Kaw et Roura)	French Guiana	FGU	X	X		
MHNG	1978_076	V-2879	M	*P. rubiginosus*	Regina, Grotte Mathilde	French Guiana	FGU	X	X	X	KF636795
MHNG	1978_077	V-2880	M	*P. alitonus*	Regina, Grotte Mathilde	French Guiana	FGU	X	X	X	KF636809
MHNG	1978_078	V-2899	M	*P. alitonus*	Regina, Grotte Mathilde	French Guiana	FGU	X	X	X	KF636811
MHNG	1978_079	V-2900	F	*P. rubiginosus*	Regina, Grotte Mathilde	French Guiana	FGU	X	X	X	KF636797
MHNG	1978_080	V-2901	F	*P. rubiginosus*	Regina, Grotte Mathilde	French Guiana	FGU	X	X	X	KF636798
MHNG	1978_081	V-2902	M	*P. alitonus*	Regina, Grotte Mathilde	French Guiana	FGU	X	X	X	KF636810
MHNG	1978_082	V-2903	M	*P. alitonus*	Regina, Grotte Mathilde	French Guiana	FGU	X	X	X	KF636805
MHNG	1978_083	V-2904	M	*P. rubiginosus*	Regina, Grotte Mathilde	French Guiana	FGU	X	X	X	KF636796
MHNG	1978_084	V-2905	F	*P. rubiginosus*	Regina, Grotte Mathilde	French Guiana	FGU	X	X	X	KF636794
MHNG	1978_085	V-2906	M	*P. alitonus*	Regina, Grotte Mathilde	French Guiana	FGU	X	X	X	KF636807
MHNG	1978_086	V-2907	M	*P. alitonus*	Regina, Grotte Mathilde	French Guiana	FGU	X	X	X	KF636806
MHNG	1978_087	V-2908	M	*P. alitonus*	Regina, Grotte Mathilde	French Guiana	FGU	X	X	X	KF636812
MHNG	1978_088	V-2909	F	*P. rubiginosus*	Regina, Grotte Mathilde	French Guiana	FGU	X	X	X	KF636793
MHNG	1978_089	V-2910	F	*P. alitonus*	Regina, Grotte Mathilde	French Guiana	FGU	X	X	X	KF636808
MHNG	1979_073	V-2941	M	*P. rubiginosus*	Cacao: Va-Joua	French Guiana	FGU	X	X		
MHNG	1980_093	V-2969	M	*P. alitonus*	Réserve Trinité: AYA	French Guiana	FGU	X	X		
MHNG	1980_094	V-2981	F	*P. alitonus*	Kaw: Grotte Mathilde	French Guiana	FGU	X	X		
MHNG	1983_043	V-3073	M	*P. alitonus*	Cacao	French Guiana	FGU	X	X		
MHNG	1983_058	V-3088	M	*P. alitonus*	Cacao	French Guiana	FGU	X	X		
MHNG	1983_064	V-3094	M	*P. rubiginosus*	Cacao	French Guiana	FGU	X	X		
MHNG	1983_065	V-3095	M	*P. rubiginosus*	Cacao	French Guiana	FGU	X	X		
MHNG	1983_069	V-3099	M	*P. alitonus*	Cacao	French Guiana	FGU	X	X		
MHNG	C1228		U	*P. alitonus*	Montagne de Gouffres, Kaw	French Guiana	FGU			X	KX590097
MHNG	C1229		U	*P. alitonus*	Montagne de Gouffres, Kaw	French Guiana	FGU			X	KX590098

VN	FN	S	Species	Locality	Country	Population	M	A	*COI*	GN
MHNG	C1230	U	*P. alitonus*	Montagne de Gouffres, Kaw	French Guiana	FGU			X	KX590099
TTU	110311	TK151456	M	*P. alitonus*	Sipaliwini	Suriname	SUR			X	KX590264
TTU	106014	TK145282	M	*P. rubiginosus*	Sipaliwini	Suriname	SUR			X	KX590259
TTU	106023	TK145283	F	*P. rubiginosus*	Sipaliwini	Suriname	SUR			X	KX590260
TTU	106024	TK145284	M	*P. alitonus*	Sipaliwini	Suriname	SUR			X	KX590261
TTU	106025	TK145285	F	*P. rubiginosus*	Sipaliwini	Suriname	SUR			X	KX590262

Appendix II

List of specimens examined. This list refers to all specimens included in the morphological study regardless if they were included or not in the morphometric analysis. AMNH = American Museum of Natural History; IEPA = Instituto de Pesquisas Científicas e Tecnológicas do Estado do Amapá; INPA = Instituto Nacional de Pesquisas da Amazônia; MHNG = Musée d'Histoire Naturelle – Genève; MPEG = Museu Paraense Emílio Goeldi; MZUSP = Museu de Zoologia da Universidade de São Paulo; ROM = Royal Ontario Museum.

Pteronotus alitonus sp. nov. (n = 82).—**BRAZIL**:–Amapá: Rio Cupixi, Reserva de Iratapuru, Pedra Branca do Amapari, 0.58N 52.32W (IEPA 380, 415, 417); Parque Nacional Montanhas do Tumucumaque, Rio Anoteie, Oiapoque, 3.22N 52.02W (IEPA 456); Rio Jari, Laranjal do Jari, 0.62S 51.52W (IEPA 1833, 1843, 1847, 1853, 1893). Amazonas: Caverna Maroaga Km 6 - Usina Hidrelétrica Balbina, Manaus, 2.04S 59.95W (INPA 332, 339, 343, 345, 351, 358, 359, 361); Estrada S-2, Usina Hidrelétrica Balbina, margem direita do rio Uatumã, Manaus, 1.94S 59.48W (INPA 515, 529, 888, 964B); Igarapé Caititu, margem direita do rio Uatumã, 20 Km da foz, 2.61S 58.15W (INPA 1361, 1362, 1363, 1365); Reserva Biológica do Cuieiros, Base de Apoio ZF-2, Manaus, 2.59S 60.21W (INPA 2ZFII03, 2ZFII10); Manaus, 80 km N, 2.41S 59.88W (INPA 6942, 6945, 6947, 6948, 6949, 6950, 6952, 6954). Pará: Itaituba, 6.05S 56.30W (MPEG 41678, MZUSP 35503, 35504, 35505). **FRENCH GUIANA**:–Cayenne: Sinnamary, Paracou, 5.38N 52.95W (AMNH 267851, 267405, 267406). Régina: Grotte Mathilde, 4.52N 52.12W (MHNG 1972.051, 1978.077, 1978.078, 1978.081, 1978.082, 1978.085, 1978. 086, 1978.087, 1978.089, 1980.094). Roura: Cacao, 4.57N 52.45W (MHNG 1983.043, 1983.058, 1983.069); Trésor Natural Preservation, 4.62N 52.28W (MHNG 1972.052). Saint Elie: La Trinité, 5.02N 53.66W (MHNG 1980.093). **GUYANA**:–East Berbice-Corentyne: Mango Landing, Corentyne River, 5.17N 57.3W (ROM 100427). Potaro-Siparuni: Amaila Falls, 5.52N 59.26W (MZUSP 35518, 35520, 35521, 35522, 35523, 35524, 35525, 35526, 35527, 35529); Iwokrama Reserve, 25 km SSW of Kurupukari, 4.47N 58.78W (ROM 104705). Upper Demerara-Berbice: Kurupukari, East Bank, Essequibo River, 4.67N 58.68W (ROM 98128); Tropenbos, 20 km SSE of Mabura Hill, 5.15N 58.7W (ROM 103374). Upper Takutu-Upper Essequibo: Chodikar River, 55 km SW of Gunn's Strip, 1.37N 58.77W (ROM 106585); Gunn's Strip, 1.65N 58.63W (ROM 106776); 5 km SE of Surama, 4.1N 59.05W (ROM 102973); Kamoa River, 50 km SWW of Gunn's Strip, 1.54N 58.85W (ROM 106659). **SURINAME**:–Sipaliwini: Iconja Landing, Sipaliwini River, 1.99N 56.09W (ROM 120275, 120294); Kutari River Camp, 2.18N 56.79W (ROM 120589); Sipaliwini River Camp, 2.29N 56.61W (ROM 120631, 120645); Blanche Marie Vallen, 4.76N 56.88W (ROM 117576); Bakhuis, Area 8 Recon Fly Camp, 4.45N 56.86W (ROM 117545).

Pteronotus rubiginosus (n = 102).—**BRAZIL**:–Amapá: Rio Cupixi, Reserva de Iratapuru, Pedra Branca do Amapari, 0.58N 52.32W (IEPA 418, 428); Parque Nacional Montanhas

do Tumucumaque, Rio Anoteie, Oiapoque, 3.22N 52.02W (IEPA 476); Parque Nacional Montanhas do Tumucumaque, Rio Mutum, Calçoene, 1.39N 51.93W (IEPA 525, 533, 550, 554); Fazenda Aricari/BR156, km 147, Tartarugalzinho, 0.95N 51.25W (IEPA 722, 748, 758, 760). Amazonas: Caverna Maroaga Km 6 - Usina Hidrelétrica Balbina, Manaus, 2.04S 59.95W (INPA 333, 353); Manaus, 80 km N, 2.41S 59.88W (INPA 6941, 6943, 6944, 6946, 6951, 6955); Paca-Mirim, margem direita Rio Abacaxis, 4.59S 58.22W (LM-ABX58); Reserva Biológica do Cuieiros, Base de Apoio ZF-2, Manaus, 2.59S, 60.21W (INPA 2ZFII15). Mato Grosso: Cuiabá, 15.72S 55.77W (35151, 35152); Jangada, 15.27S 55.22W (MZUSP 35147, 35148, 35149, 35150); Pontes Larcerda, 15.2S 59.37W (MZUSP 29504); Ribeirãozinho, 16.49S 52.7W (MZUSP 35514, 35515); Rondonópolis, 16.25S 54.15W (MZUSP 35513); São Vicente, 15.82S 55.4W (MZUSP 35153, 35154, 35155); Serra das Araras, 15.48S 57.19W (MZUSP 35702, 35703, 35704, 35705, 35706, 35707). Pará: Floresta Nacional Tapirapé-Aquiri, Marabá, 5.78S 50.54W (MPEG 38809, 38828, MZUSP 35506, 35507, 35508, 35509, 35510, 35512). Piauí: Estação Ecológica Uruçui-Una, Bom Jesus, 8.83S 44.17W (MZUSP 30035, 30120, 30142, 30155, 30210, 30226). Rondônia: Rio Madeira, margem esquerda, módulo Ilha das Pedras, Porto Velho, 9.16S 64.63W (INPA 6085, 6093, 6100, IF26); Rio Madeira, módulo Jirau margem direita, Porto Velho, 9.16S 64.71W (INPA JRDA27); Rio Jaci-Parana, Porto velho - margem direita do rio madeira, 9.45S 64.37W (INPA 6116, 6120, 6129, JCDF35); Usina Hidrelétrica Jirau, 9.44S 64.82W (MZUSP 35511, 35516, 35517); Vilhena, 12.72S 60.26W (MZUSP 35699, 35700, 35701). **FRENCH GUIANA**:–Cayenne: Sinnamary, Paracou, 5.38N 52.95W (AMNH 267283, 267284, 267285, 267286, 267288, 269115). Régina: Grotte Mathilde, 4.52N 52.12W (MHNG 1978.076, 1978.079, 1978.080, 1978.083, 1978.084, 1978.088). Roura: Cacao, 4.57N 52.45W (MHNG1983.064, 1983.065, 1979.073); Trésor Natural Preservation, 4.62N 52.28W (MHNG 1972.050). **GUYANA**:–East Berbice-Corentyne: Mango Landing, Corentyne River, 5.17N 57.3W (ROM 100391, 100397). Potaro-Siparuni: Amaila Falls, 5.52N 59.26W (MZUSP 35519, 35528). Upper Demerara-Berbice: Kurupukari, East Bank, Essequibo River, 4.67N 58.68W (ROM 98127); Tropenbos, 20 km SSE of Mabura Hill, 5.15N 58.7W (ROM 103375, 103420). Upper Takutu-Upper Essequibo: Annai, 3.95N 59.13W (ROM 97963, 97964); Chodikar River, 55 km SW of Gunn's Strip, 1.37N 58.77W (ROM 106575); 5 km SE of Surama, 4.1N 59.05W (ROM 102991); Karanambo, 3.75N 59.3W (ROM 97957). **SURINAME**:–Sipaliwini: Sipaliwini Village, 2.03N 56.12W (ROM 120408); Blanche Marie Vallen, 4.76N 56.88W (ROM 117608, 117654); Bakhuis, transect 13, 4.55N 57.06W (ROM 117282); Bakhuis, Transect 14, 4.58N 57.05W (ROM 117338).

Pteronotus fuscus (n = 15).—**GUYANA**:–Barima-Waini: Baramita, Old World, 7.36N 60.48W (ROM 100871, 100948, 101046). **VENEZUELA**:–Aragua: Rancho Grande, 10.37N 67.68W (AMNH 144842, 144845); Carabobo: San Esteban, 10.43N 68.02W (AMNH 31565, 31566, 31568, 31569, 31570, 31571, 31576); Las Quigas, 10.40N 68.00W (AMNH 31561, 31563, 31564).